Title

The late Mesozoic–Cenozoic tectonic evolution of the South China Sea: A petrologic perspective

Authors

Yan, Quanshu
Shi, Xuefa
Castillo, Paterno R

Publication Date

2014-05-01

DOI

10.1016/j.jseaes.2014.02.005

Peer reviewed

Journal of Asian Earth Sciences 85 (2014) 178–201

Contents lists available at ScienceDirect

Journal of Asian Earth Sciences

journal homepage: www.elsevier.com/locate/jseaes

Review

The late Mesozoic–Cenozoic tectonic evolution of the South China Sea: A petrologic perspective

Quanshu Yan [a], Xuefa Shi [a,*], Paterno R. Castillo [b]

[a] Key Laboratory of Marine Sedimentary and Environmental Geology, The First Institute of Oceanography, State Oceanic Administration, Qingdao 266061, China
[b] Scripps Institution of Oceanography, UCSD, La Jolla, CA 92093, USA

ARTICLE INFO

Article history:
Received 12 November 2013
Received in revised form 24 January 2014
Accepted 7 February 2014
Available online 14 February 2014

Keywords:
Late Mesozoic era
Cenozoic
Igneous rocks
Tectonic evolution
South China Sea

ABSTRACT

This paper presents a review of available petrological, geochonological and geochemical data for late Mesozoic to Recent igneous rocks in the South China Sea (SCS) and adjacent regions and a discussion of their petrogeneses and tectonic implications. The integration of these data with available geophysical and other geologic information led to the following tectono-magmatic model for the evolution of the SCS region. The geochemical characteristics of late Mesozoic granitic rocks in the Pearl River Mouth Basin (PRMB), micro-blocks in the SCS, the offshore continental shelf and Dalat zone in southern Vietnam, and the Schwaner Mountains in West Kalimantan, Borneo indicate that these are mainly I-type granites plus a small amount of S-type granites in the PRMB. These granitoids were formed in a continental arc tectonic setting, consistent with the ideas proposed by Holloway (1982) and Taylor and Hayes (1980, 1983), that there existed an Andean-type volcanic arc during later Mesozoic era in the SCS region. The geochonological and geochemical characteristics of the volcanics indicate an early period of bimodal volcanism (60–43 Ma or 32 Ma) at the northern margin of the SCS, followed by a period of relatively passive style volcanism during Cenozoic seafloor spreading (37 or 30–16 Ma) within the SCS, and post-spreading volcanism (tholeiitic series at 17–8 Ma, followed by alkali series from 8 Ma to present) in the entire SCS region. The geodynamic setting of the earlier volcanics was an extensional regime, which resulted from the collision between India and Eurasian plates since the earliest Cenozoic, and that of the post-spreading volcanics may be related to mantle plume magmatism in Hainan Island. In addition, the nascent Hainan plume may have played a significant role in the extension along the northern margin and seafloor spreading in the SCS.

Contents

* Corresponding author. Address: Key Laboratory of Marine Sedimentary and Environmental Geology, The First Institute of Oceanography, State Oceanic Administration, No. 6, Xianxialing Road, Laoshan district, Qingdao 266061, China. Tel.: +86 532 88961651; fax: +86 532 88967491.
E-mail address: shixuefa@163.com (X. Shi).

http://dx.doi.org/10.1016/j.jseaes.2014.02.005
1367-9120/

1. Introduction

The South China Sea (SCS) is one of the largest marginal basins in the western Pacific. Since the Paleozoic era, the SCS and adjacent regions (henceforth termed the SCS region) experienced a complex tectonic evolution. As an important part of southeast Asia, the SCS region has been the focus of numerous Paleozoic and Mesozoic palaeogeographic reconstructions (e.g., Karig, 1971; Hamilton, 1979; Taylor and Hayes, 1983; Tapponnier, 1986; Yan and Shi, 2007; Hall et al., 2008; Zhou et al., 2008; Metcalfe, 2010; Morley, 2012; and references therein). Based on tectonostratigraphic, palaeobiogeographic and palaeomagnetic data, Metcalfe (1996, and references therein) suggested that the various pre-Cretaceous continental terranes of east and southeast Asia were all derived directly or indirectly from Gondwanaland and the northward drift of these terranes was accompanied by the opening and closing of three successive oceans - the Palaeo-Tethys, Meso-Tethys and Ceno-Tethys. In his tectonic evolution model, there existed a marginal basin (named the Proto-South China Sea) in late Cretaceous time that finally closed at the northwest Palawan trough by its subduction towards the Philippines and Borneo (Cullen, 2013).

During the Cenozoic era, the tectonic evolution of the SCS region was influenced by the collision between Indo-Australian and Eurasian plates and the ocean-ward retreat of the subduction zone of the Pacific plate (Lee and Lawver, 1994; Honza, 1995; Honza and Fujioka, 2004; Hall, 1996, 2002; Hall et al., 2008, 2009). Based on seafloor magnetic anomalies, Taylor and Hayes (1980, 1983) suggested that the seafloor spreading period in the SCS was at 32–17 Ma, but this was subsequently adjusted to 32–15.5 Ma by Briais et al. (1993), and further revised to 30–16 Ma based on the time scale of Cande and Kent (1995). Barckhausen and Roeser (2004) interpret cessation of SCS spreading at 20.4 Ma. A recent study, however, showed that the time for initial spreading could be as old as 37 Ma (magnetic anomaly C17) (Hsu et al., 2004). The spreading mode and dynamic setting of the SCS is currently still in debate (e.g., Karig, 1971; Taylor and Hayes, 1980, 1983; Tapponnier, 1986; Briais et al., 1993; Li et al., 1998; Yan and Shi, 2007).

Igneous activity plays an important role in plate reconstruction and regional tectonic evolution. In previous reconstructions of the SCS region, however, few petrological data were included. Zhou et al. (2005) and Yan et al. (2006) systematically summarized the temporal–spatial distribution of Mesozoic–Cenozoic magmatism in the region, but detailed petrogenetic discussions were not presented. The publication of new petrological data can provide a better understanding of the igneous activity in the region. The objective of this paper is to review recently published petrological

data and discuss their petrogenetic significance and implications for the tectonic evolution of the SCS region. This paper focuses on igneous rocks that predominantly indicate the tectonic setting, whereas metamorphic and sedimentary rocks (e.g., metamorphic and meta-sedimentary rocks in Dangerous Grounds and ophiolitic rocks - Hutchison, 2005) representing ancient sutures widely distributed in northwestern Borneo are not included in this study.

2. Geological setting

The SCS lies at the intersections of the Eurasian plate, Philippine Sea plate and Indo-Australian plate (Fig. 1) and, thus, its geology had been greatly affected by these surrounding lithospheric plates. The SCS can be subdivided into three parts, the northern continental margin, the ocean basin and the southern continental margin. The major geological features defining the SCS include the east Vietnam fault in the west, the NW Palawan Trough in the south, the Manila trench in the east, and a transition(?) zone in the north.

The northern margin of the SCS (Figs. 2 and 3), which lies between the South China fold belt and continent to ocean boundary (COB) of the SCS, consists of several extensional basins including the Sanshui, Lianping, Heyuan, Pearl River Mouth, southwest Taiwan, and Qiongdongnan basins that developed since early Cenozoic (e.g., Zou et al., 1995; Chung et al., 1997; Li et al., 1998, 1999; Zhou et al., 2009 and references therein). The eastern margin of the SCS is a subduction zone, where the SCS Basin crust formed during the Cenozoic seafloor spreading is subducting eastwards beneath the Philippine Sea plate, forming a volcanic arc along the western margins of the islands of Luzon and Taiwan (Defant et al., 1989, 1990). The southern margin of the SCS is also a compressive collision zone, where the subduction of the proto-South

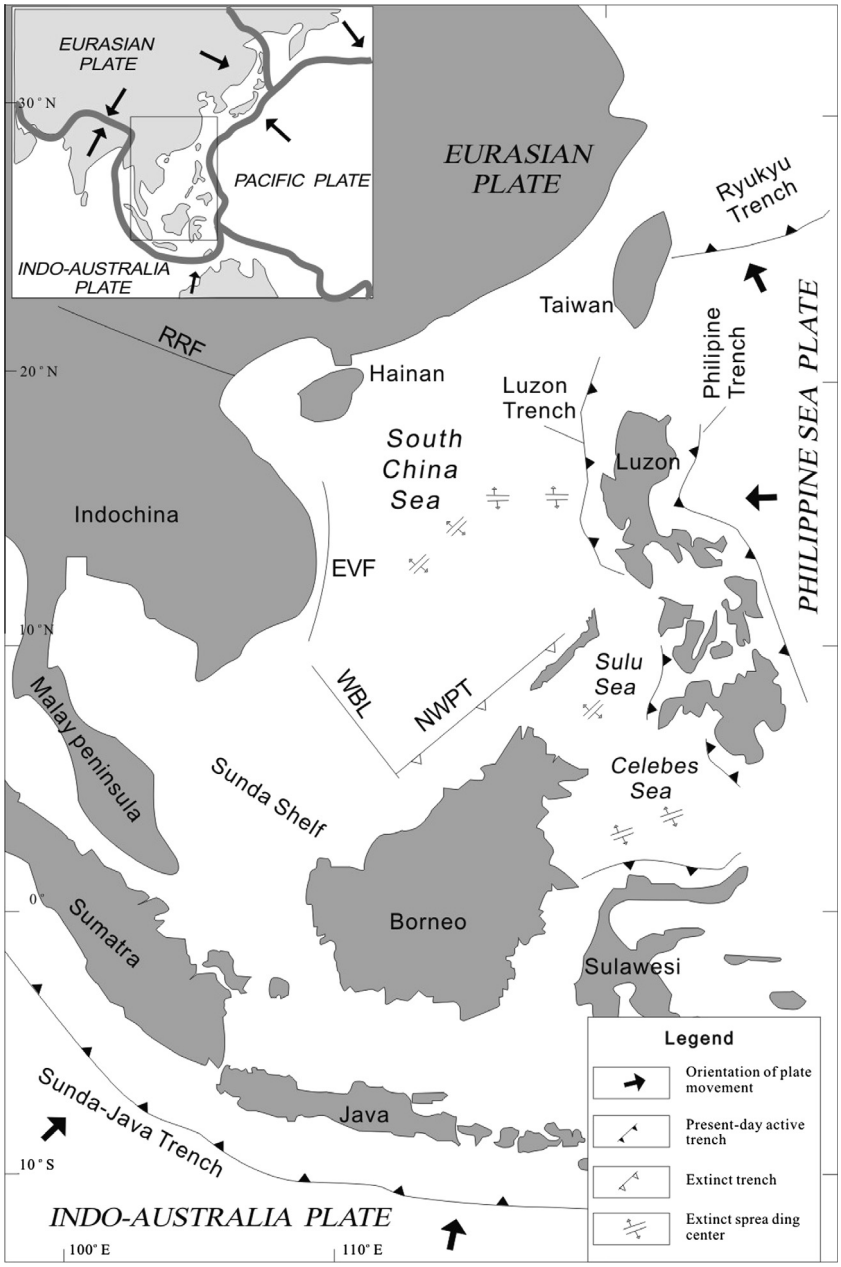

Fig. 1. Simplified geologic map of the South China Sea and adjacent region. Inset figure show major tectonic plates surrounding the SCS. EVF – East Vietnam Fault. RRF – Red River Fault; WBL – West Baram Line; NT – Nansha Trough; NWPT – Northwest Palawan Trough.

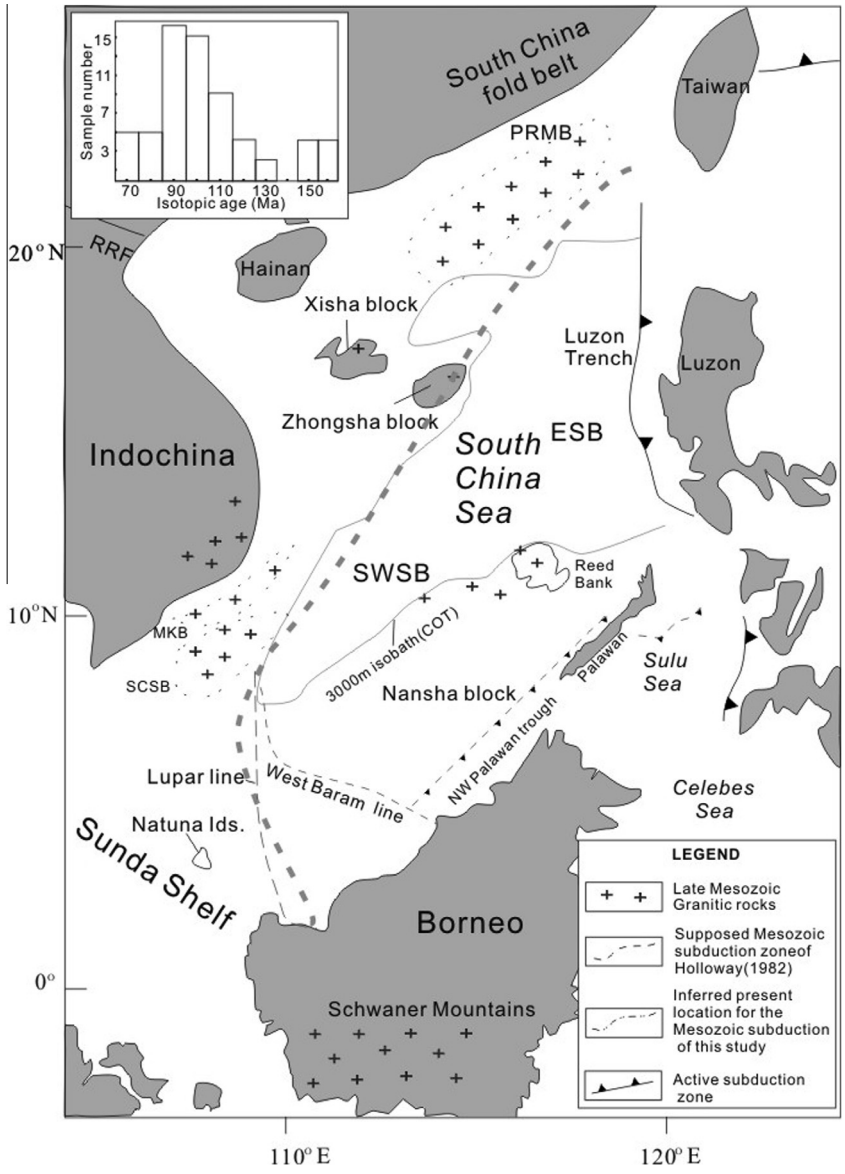

Fig. 2. Sketch map for the distribution of late Mesozoic granitic rocks in the SCS region. Inset figure is the histogram of distribution of ages for late Mesozoic granitic rocks from the SCS region. The late Mesozoic subduction zone proposed by Holloway (1982) and Hall (2012) were also shown. MKB – Mekong Basin; NWSB – Northwest Sub-basin; PMB – Pearl River Mouth Basin; RRF – Red-River Fault; SCSB – South Con Son Basin; SWSB – Southwest Sub-basin; COB – Continent–Ocean boundary; PCT – Palawan Continental Terrane (Knittel et al., 1995). Xisha Ids., Zhongsha Ids. Nansha Ids. and Natuna Ids. represent Xisha Islands, Zhongsha Islands, Nansha Islands and Natuna Islands, respectively.

China Sea crust beneath the island of Borneo occurred due to the collision between the leading edge of the Indo-Australian plate and Sundaland or the anticlockwise rotation of Borneo (Hall, 1996). Recent paleomagnetic data from NW Borneo call into question the anticlockwise rotation of a rigid Borneo during the Miocene (Cullen et al., 2012). The compressional stress field in the northwest Palawan trough (i.e., Nansha Trough in Chinese, Hamilton, 1979; Hutchison, 2004, 2005; Hutchison and Vijayan, 2010) and onland Borneo region (Tingay et al., 2010) appears to have recorded the subduction of the proto-SCS crust. Finally, the western margin of the SCS is a strike-slip and pull-apart region, where a series of oil (and gas) -bearing basins developed. The East Vietnam fault (EVF) is a major controlling structure in this region, and its relationship to the Red-River fault is not clear. The accurate interpretation of the nature of EVF and its southward extension will constrain whether the far-field effect of the India–Asian collision in the earliest Cenozoic has reached Borneo or not (Tapponnier, 1986; Hall et al., 2008; Clift et al., 2008; Morley, 2012, 2013).

The oceanic SCS basin is outlined roughly by the 3000 m isobath from surrounding areas, and is subdivided into northwest, east and southwest sub-basins. The overall timing of seafloor spreading in the basin, i.e., its initiation in late Eocene–early Oligocene shortly after the collision between India and Eurasian plate and its cessation during the collision between the leading edge of Indo-Australian plate and Sundaland, had already been constrained by several authors (e.g., Taylor and Hayes, 1983; Tapponnier, 1986; Briais et al., 1993). However, spreading within the southwest sub-basin remains controversial (Taylor and Hayes, 1983; Ru and Piggot, 1986; Lu, 1987; He, 1988; Briais et al., 1993). Based on geophysical data, the crustal thickness of the whole SCS basin crust and lower part of continental slope are 8–12 km and 10–20 km, respectively, and the elastic thickness of the basin crust is less than 6 km

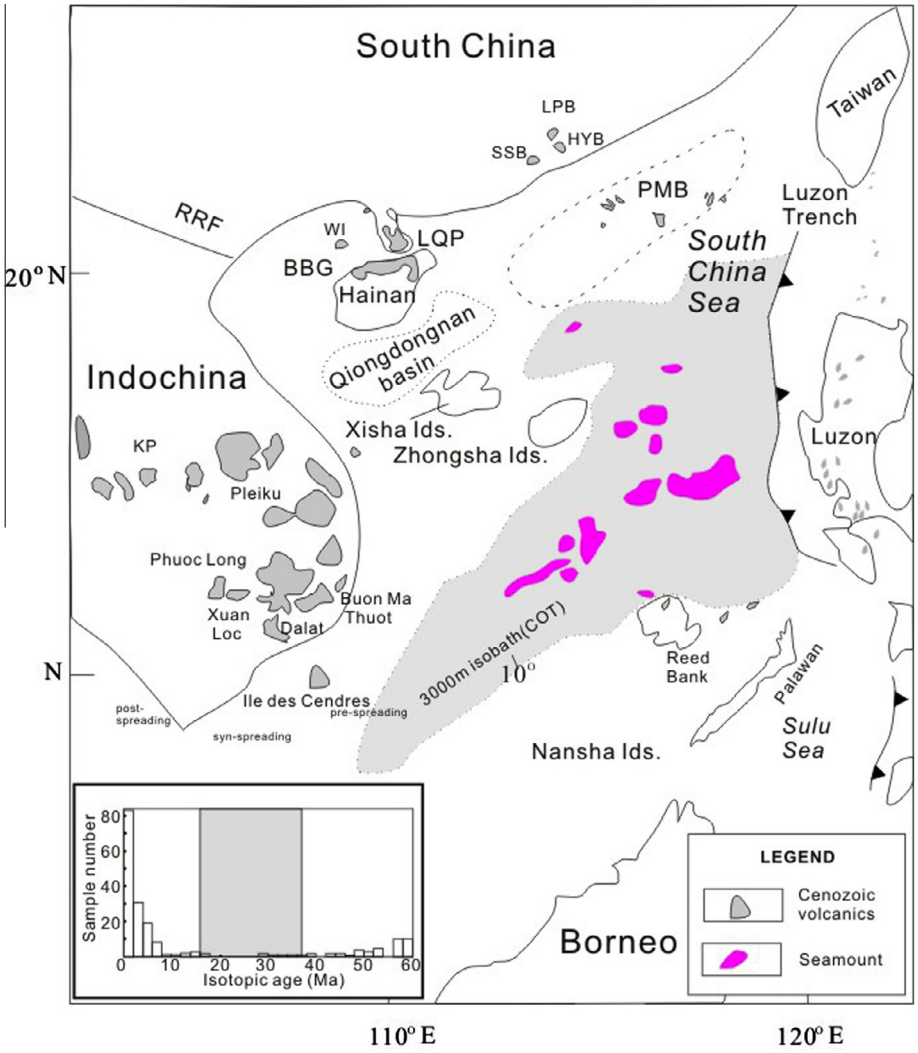

Fig. 3. Sketch map for the distribution of Cenozoic volcanics in the SCS region. Inset figure is the histogram of distribution of ages for Cenozoic volcanics from the SCS region. BBG – Beibu Gulf; HYB – Heyuan Basin; KP – Khorat Plateau (Thailand); LPB – Lianping Basin; LQP – Leiqiong Peninsula; PRMB – Pearl River Mouth Basin; SSB – Sanshui Basin; WI – Weizhou Island; RRF – Red-River Fault; COB – Continent–Ocean Boundary. Seamounts area is defined by the area above the 3000 isobath in the ocean basin.

(Braitenberg et al., 2006). In addition, volcanic seamounts which formed after the cessation of the seafloor spreading are widely distributed in the basin (Tu et al., 1992; Yan et al., 2008a,b).

Although their exact number is controversial, there are also several micro-continental blocks dispersed within the SCS (Fig. 1), e.g., Zhongsha block (Macclesfield Bank), Xisha block (Paracel Islands), Dongsha block (Pratas Reef) (?), Nansha block (Spratly Islands), and possibly the west Luzon basin that is converging with Luzon island (e.g., Liu et al., 2002, 2011; Yao et al., 2004; Arfai et al., 2011). Among these blocks, the Nansha micro-block is relatively well-studied, and its geology may be representative of all the micro-blocks in the SCS. Like the other blocks, the crust of the Nansha micro-block is relatively thin (Hamilton, 1979; Hinz and Schlüter, 1985), varying from 16 to 25 km (Yao et al., 2004). Hutchison and Vijayan (2010) suggested that all the islands in this micro-block are covered by coral reefs, and the basement rocks reported by Kudrass et al. (1986) and Yan et al. (2008c, 2010) have been dredged from its cuestas (Hutchison and Vijayan, 2010). The micro-blocks, together with Hainan Island, were regarded as parts of a single block, i.e., the "Qiongnan" block, during paleo-Tethys times (e.g., Liu et al., 2002, 2011; Yao et al., 2004). The Qiongnan block was inferred to have a Proterozoic folded continental basement (e.g., Liu et al., 2002; Yan et al., 2010) and had an affinity to the South China block based on geophysical (e.g., Liu et al., 2006), and Pb isotopic data (Yan et al., 2011). The current micro-blocks were rifted from each other since the end of late Mesozoic, and ceased drifting as a result of the collision of these blocks with NW Borneo (e.g., Taylor and Hayes, 1980, 1983; Holloway, 1982; Kudrass et al., 1986; Jin, 1989; Schluter et al., 1996; Hall, 2002, 2012; Yao et al., 2004; Liu et al., 2006; Knittel, 2011). In addition, Hall et al. (2009, 2012) recently suggested that these micro-blocks once were a single, large block named "Luconia-Dangerous Grounds", which belonged to Sundaland (Hutchison and Vijayan, 2010) and separated from each other due to rifting and spreading in the SCS (cf., Metcalfe, 2011a).

3. Igneous activity in the SCS region

Zhou et al. (2005) and Yan et al. (2006) had summarized the temporal–spatial distribution of Mesozoic–Cenozoic magmatism in the SCS region, but they mainly focused on Cenozoic igneous rocks. Moreover, they did not discuss the petrogeneses of and the relationships between these rocks. In this study, we combine recently published petrologic, geochemical and geochronologic data with tectonic and geophysical data in order to develop a model

for the tectono-magmatic evolution of the SCS region from the Mesozoic to Recent.

3.1. Late Mesozoic igneous activity

Late Mesozoic igneous activity widely occurred in east and southeast Asia. Many authors tend to invoke the subduction of the old Pacific plate beneath the Eurasian plate to account for the widespread late Mesozoic Yanshanian igneous rocks in east China (e.g., Jahn, 1974; Jahn et al., 1990; Lan et al., 1996; Wu et al., 2005; Li et al., 2007; Li and Li, 2007 and references therein). In the SCS region, contemporaneous late Mesozoic igneous activities have been reported, e.g., the Pearl River mouth basin (Li and Rao, 1994; Li et al., 1999), Zhongsha micro-block (Jin, 1989), Nansha micro-block (Dangerous Grounds or Spratly Islands) (Yan et al., 2008c, 2010), northern Mindoro (part of the Palawan Continental terrane) (Knittel, 2011), southeastern Vietnam (Hamilton, 1979; Nguyen et al., 2004a,b) and its offshore continental shelf (Areshev et al., 1992), and West Kalimantan, Borneo (Williams et al., 1988) (Fig. 2). The ages obtained for these Late Mesozoic igneous rocks from the SCS region range from 159 Ma (the Nansha block) to 70.5 Ma (PRMB), implying that the Late Mesozoic igneous activities in the SCS region span a long time. The lithologies of these Late Mesozoic igneous rocks are variable, but their geochemical data show that these rocks, similar to those from east or southeast China (e.g., Zhou and Li, 2000; Wu et al., 2005), are related to the subduction zone setting. The details including sampling location, lithology and geochronology of rock samples are listed in Table 1.

3.1.1. Pearl River mouth basin (PRMB)

The PRMB is a Tertiary oil- and gas- bearing basin covered by a thick layer of sediments (Li and Rao, 1994). A large portion of its basement consists of Yanshanian intermediate to silicic igneous rocks (Li et al., 1999), which have been encountered in >20 exploration and evaluation wells drilled in the basin. The majority of samples are granites; other minor rock types include granodiorite, diorite, quartz diorite, and quartz monzonite. Most of the samples have cataclastic texture, which may indicate that the granitic batholith underwent later tectono-thermal deformation and/or burial metamorphism due to the weight of overlying sediments. The samples were dated 153–70.5 Ma, with an average value of ~100 Ma, (Li et al., 1999; Table 1); these correspond to the ages of Taiwan granites (Lan et al., 1996), but are younger than granites in southeast China (e.g., Li, 2000; Zhou and Li, 2000). It is noteworthy that for the same sample, the Rb/Sr age is younger than K/Ar age (a problem of Argon excess), suggesting that Rb–Sr isotopic ages (whole rock isochrons) had been affected by later geological events.

3.1.2. Micro-blocks in the SCS

Dioritic rocks had been dredged from the Zhongsha bank, Xisha micro-block and continental slope in the northern margin of the SCS (Jin, 1989). These rocks mainly consist of plagioclase, hornblende and pyroxene, and minor magnetite and apatite. Because the samples had been strongly hydrothermally alterated, their age could not be accurately determined. However, the age range of biotite–plagioclase gneiss from the basement of the northeastern end of Zhongsha block is 119 Ma (K–Ar dating method of plagioclase) to 127 Ma (K–Ar dating method of biotite) (Jin, 1989). These ages correspond to the early Cretaceous igneous activity in east China (e.g., Jahn et al., 1990; Zhou and Li, 2000).

Some granitic samples were dredged from two locations at the COB in the northern margin of the Nansha micro-block (Yan et al., 2008c). These include tonalite, monzogranite and granodiorite. Tonalite and granodiorite consist of quartz, plagioclase, K-feldspar, biotite, and hornblende whereas monzogranite consists of plagioclase, K-feldspar, quartz, and biotite. Four representative samples range from 159 to 127 Ma (Zircon U–Pb dating method), corresponding well to the ages of granites in southeast China (e.g., Jahn et al., 1990; Zhou and Li, 2000; Wu et al., 2005).

Jurassic–Cretaceous metamorphic rocks were dredged from Reed Bank and Dangerous Grounds (Kudrass et al., 1986). The K–Ar ages of these samples are 146 Ma for an amphibolite, 122 Ma for a paragneiss and 113 Ma for a garnet–mica schist and quartz phyllite, respectively. Petrographically most of these rocks were derived or metamorphosed from sediment or sedimentary rocks, so they may not represent the true basement but sedimentary cover or the products of later sedimentation. Interestingly, older (Triassic) sediments have been dredged from the region-possible protolith (Kudrass et al., 1986). Nevertheless, they are at least contemporaneous to the Yanshanian tectonic and thermal event mentioned above.

3.1.3. Southeastern Vietnam and its continental shelf

The basement rock of the Dalat zone in southern Vietnam, which is part of the Indochina block, is part of the Precambrian Kontum massif (Lan et al., 2003) and is emplaced by the following three plutons, i.e., the Dinhquan, Cana and Deoca granitoid suites (Nguyen et al., 2004b). The Dinhquan suite is composed of hornblende–biotite granodiorites, diorites, and minor granites; the granodiorite was dated 112–100 Ma (zircon U–Pb dating method). The Cana suite consists of biotite-bearing granites, and a granite sample was dated 93–96 Ma (zircon U–Pb dating method). The Deoca suite consists of granodiorites, monzogranites and diorites, and one sample was dated 88–92 Ma (zircon U–Pb dating method). The ages of the granitic rocks in southern Vietnam obtained by Nguyen et al. (2004b) are basically similar to those in Taiwan (Lan et al., 1996), and are younger than the Cretaceous granites in southeast China (e.g., Li, 2000) and Nansha micro-block (Yan et al., 2008c).

The basement rocks of the continental shelf in southern Vietnam also belong to the Indochina block and consist mainly of granites and granodiorites (Areshev et al., 1992) that are petrographically similar to the basement rocks in PRMB (Li et al., 1999). As in the PRMB, these granitic rocks were severely alterated during later tectonic-hydrothermal events and/or burial metamorphism of overlying sediment. Interestingly the fractured granitic rocks are a good oil reservoir (Areshev et al., 1992; Cuong and Warren, 2009). In the Mekong basin, the basement age (K–Ar dating method of biotite) was determined to be at 178–108 Ma for granite, 149–135 Ma for granodiorite and 97 Ma for quartz diorite. In the South Con Son Basin, the basement rock was dated at 105–109 Ma for granodiorite (Areshev et al., 1992; Nguyen et al., 2004b). The basement age range in this area is the largest in the SCS region and needs to be further constrained by high-resolution dating methods.

3.1.4. West Kalimantan (Borneo)

West Kalimantan (Borneo) can be divided into the Schwaner Mountains, the NW Kalimantan block and the Northern belt. The NW Kalimantan block granitoids were dated 320–204 Ma and the Northern belt granites 80–75 Ma by K–Ar biotite or hornblende dating method (Williams et al., 1988). For the ~east–west trending Schwaner Mountain granitoids, Haile et al. (1977) obtained K–Ar biotite and hornblende ages ranging from 157 Ma to 77 Ma whereas Williams et al. (1988) obtained tighter and more reliable K–Ar biotite or hornblende ages ranging from 123–86 Ma for tonalite–syenogranite and potassic granites. The later ages are comparable with those of Taiwan granites (e.g., Lan et al., 1996), offshore continental shelf (Areshev et al., 1992) and Dalat zone (Nguyen et al., 2004b) in Southern Vietnam, generally supporting the notion that there was once a continuous Mesozoic east Asia magmatic arc.

Table 1
Data for late Mesozoic granitic rocks from the SCS region. *Mineral Abbreviations:* am – amphibole; bt – biotite; hbl – hornblende; mu – muscovite; mc – microcline; pl – plagioclase; qtz – quartz; zrn – zricon. *Rock Abbreviations:* D – diorite; G – Granite; GD – Granodiorite; GDP – Granodiorite porphyry; MZ – monzonite; MZG – Monzogranite; PG – Potassic granites; R – rhyolite; RP – rhyolite porphyry; SG – syengranite; T – tonalite; WR – whole rock.

	Sample Number[a]	Sample details		Lithology	Ages (Ma)	Dating method	References
		Depth (m)[b]	Longitude/latitude				
Pearl River Mouth Basin (drill cores)							
1	XJ17-3-1	2122–2124		G	79.2	K–Ar (WR)	Li et al. (1998)
2	XJ24-1-1X	3851–3851.5		G	84	K–Ar (WR)	
3	XJ24-3-1AX	4318–4319		G	98	K–Ar (WR)	
4	ZHU2	2379–2380		bt G	70.5	K–Ar (WR)	
5	ZHU1	1846–1847		G	73–76	K–Ar (WR)	
6	ZHU5	3261.8–3262.3		GDP	75	K–Ar (WR)	
7	PY3-1-1	3192		G	90.7	K–Ar (WR)	
8	PY21-3-1	4068–4069.5		bt G	89.83	K–Ar (WR)	
9	LH11-1-1A	1836.5/1822–1837.5		GD	90.62	K–Ar(WR)	
10					72.78	Rb–Sr(WR)	
11	HZ25-2-1X	3196.4		G	99.8	K–Ar (WR)	
12	HZ32-1-1	2791		G	88.5	K–Ar (WR)	
13	YJ26-1-1	1700–1702		RP	89.2	K–Ar (WR)	
14	HF28-2-1	3942–3943.6		GD	109.25	K–Ar (WR)	
15	LF2-1A	2480–2483.5		G	100.38	K–Ar(WR)	
16					94.83	Rb–Sr(WR)	
17	EP18-1-1A	3448.25		G	100.5	K–Ar (WR)	
18	PY4-1-1	3160		G	130	K–Ar (WR)	
19	PY27-1-1	3607–3609		qtz MZ	118.9	K–Ar (WR)	
20	HZ35-1-1	2218.9		qtz D	105	K–Ar (WR)	
21	SH2-1-1	3641.2		bt-hbl D	118	K–Ar (WR)	
22	KP9-1-1	1662–1774		G	153 ± 6	K–Ar (WR)	
Zhongsha Islands (dredged sample)							
23	1	Northeastern end of Zhongsha micro-block		bt-pl gneiss	126.63 ± 2.02	K–Ar(bt)	Jin (1989)
24					119.32 ± 1.91	K–Ar(pl)	
Nansha Islands (dredged samples)							
25	S08-18-2	2700	114°56′E, 11°47′N	T	159. 1 ± 1.6	U–Pb(zrn)	Yan et al. (2008c)
26	S08-18-4			T	157. 8 ± 1. 0	U–Pb(zrn)	
27	S08-32-1	3100	114°05′E, 11°28′N	MZG	153. 6 ± 0. 3	U–Pb(zrn)	
28	S08-32-2			MZG			
29	S08-32-3			MZG	127. 2 ± 0. 2	U–Pb(zrn)	
30	S08-32-4			T			
31	S08–32-5			MZG			
32	S08-32-6			T			
33	S08-32-7			MZG			
Dalat zone in southern Vietnam (land samples)							
34	DQ-8	Dinhquan suite		GD	111.6 ± 1.6	U–Pb(zrn)	Nguyen et al. (2004b)
35	DQ-1			GD	99.6 ± 1.8	U–Pb(zrn)	
36	CN-6	Cana suite		G	94.0 ± 1.1	U–Pb(zrn)	
37	CN-9			G	96.1 ± 1.1	U–Pb(zrn)	
38	CN-10			G	94.1 ± 2.1	U–Pb(zrn)	
39	CN-16			G	93.4 ± 2.0	U–Pb(zrn)	
40	DC-15	Deoca suite		G	88.0 ± 1.5	U–Pb(zrn)	
41	DC-4			G	91.3 ± 1.0	U–Pb(zrn)	
42	DC-27			G	92.0 ± 0.9	U–Pb(zrn)	
Continental shelf in southern Vietnam (drill cores)							
43	WT-67	3553.3	Mekong Basin	bt G	108	K–Ar(bt)	Areshev et al. (1992)
44	WT-91	3540.8		bt GD	149	K–Ar(bt)	
45	WT-810	3411.8		hbl-bt GD	135	K–Ar(bt)	
46	WT-402	3594.1		bt G	108	K–Ar(bt)	
47	DRAGON-3	3548.3		bt-mc G	159	K–Ar(bt)	
48	DRAGON-9	2597		bt G	178	K–Ar(bt)	
49	TAMDAO-1	3391.5		qtz D	97	K–Ar(bt)	
50	BB-2	2805.7	South Con Son Basin	mc-bt-hbl GD	109	K–Ar(bt)	
51	BB-3	3533.1		mc-bt-hbl GD	105	K–Ar(bt)	
Schwaner Mountains in west Kalimantan, Borneo (land samples)							
52	83AM109A	NW Kalimantan Block Basement	112°09′E, 0°29′N	Granitoids	320	K–Ar(hbl)	Williams et al., 1988
53	85SR217A		110°13′E, 0°33′N	Granitoids	263	K–Ar(hbl)	
54	83PW012B		110°36′E, 0°29′N	Granitoids	251	K–Ar(hbl)	
55	83PW012B		110°36′E, 0°29′N	Granitoids	201	K–Ar(bt)	
56	85FK105A		110°22′E, 0°34′N	Granitoids	214	K–Ar(bt)	
57	85RS196A		110°33′E, 0°33′N	Granitoids	211	K–Ar(bt)	
58	85PP173D		110°12′E, 0°31′N	Granitoids	204	K–Ar(hbl)	
59	83CP116B	Schwaner Mountains	111°05′E, 0°25′N	T-SG	123	K–Ar(hbl)	
60	83CP115A		111°04′E, 0°24′N	T-SG	118	K–Ar(hbl)	
61	83CP125A		111°07′E, 0°26′N	T-SG	112	K–Ar(hbl)	
62	83CP122A		111°19′E, 0°30′N	T-SG	107	K–Ar(bt)	
63	84DT003D		112°26′E, 0°57′N	T-SG	105	K–Ar(hbl)	

Table 1 (*continued*)

	Sample Number[a]	Sample details		Lithology	Ages (Ma)	Dating method	References
		Depth (m)[b]	Longitude/latitude				
64	84UM048A		112°23′E, 0°54′N	T-SG	104	K–Ar(hbl)	
65	84FK142B		110°51′E, 1°30′N	PG	91.4	K–Ar(bt)	
66	84FK101B		110°50′E, 1°35′N	PG	88.6	K–Ar(bt)	
67	84PP043A		111°00′E, 0°43′N	PG	87	K–Ar(hbl)	
68	84ER234C		110°02′E, 1°26′N	PG	86.3	K–Ar(bt)	
69	85RS160A	Northern belt	109°37′E, 2°03′N	G	80.6	K–Ar(bt)	
70	85SR064C		113°20′E, 0°45′N	G	78.6	K–Ar(bt)	
71	85UM012A		113°21′E, 0°51′N	G	78.2	K–Ar(bt)	
72	85PR078B		113°23′E, 0°43′N	G	74.9	K–Ar(hbl)	
Northern Mindoro (part of Palawan Continental Terrane) (land sample)							
73	MIN-20B			R	83	U–Pb(zrn)	Knittel (2011)

[a] Refers to sample number for land samples; well number for industrial wells or site number for dredged samples.
[b] Refers to absolute depth for granitic rocks in industrial wells, or water depth for dredged samples.

Note that the present island of Borneo suffered an anticlockwise rotation of at least 90° from its original place since Cretaceous (Fuller et al., 1999).

In addition, Knittel (2011) recently reported that there are Mesozoic (83 Ma) rhyolites in northern Mindoro (part of Palawan Continental Terrane-PCT), and he suggested that these were produced by late Yanshanian magmatism, i.e., late Mesozoic magmatism widely distributed in southeast China.

3.2. Cenozoic igneous activities

After the breakup of the SCS, some micro-blocks or a large block named Dangerous Grounds (Hall et al., 2009) began to rift and drift from the South China block, and at the same time its northern region became extended, forming a series of rifted basins. In the earliest Cenozoic, bimodal volcanism occurred in these basins (Zou et al., 1995; Zhu et al., 1989; Chung et al., 1997; Zhou et al., 2009). During Cenozoic, seafloor spreading occurred in the SCS (37 or 30–16 Ma), although only a few data about this igneous activity had been reported. After the cessation of spreading, large scale igneous activities occurred (Fig. 3) in the PRMB (Zou et al., 1995), Leiqiong peninsula (Zhu and Wang, 1989; Tu et al., 1991; Flower et al., 1992; Fan et al., 2004; Zou and Fan, 2010), Beibu Gulf (Jia et al., 2003; Li et al., 2005), Indochina block (Hoang et al., 1996; Hoang and Flower, 1998; Zhou and Mukasa, 1997; Lee et al., 1998), Reed Bank and Dangeous Grounds (Kudrass et al., 1986; Tu et al., 1992), Luzon island arc (Defant et al., 1989, 1990), and within the SCS basin itself (Wang et al., 1984; Yan et al., 2008a,b). The details including sampling location, lithology and geochronology of rock samples are listed in Table 2. In addition, there was widespread late Cenozoic calc-alkaline volcanism in central Borneo (reviewed by Zhou et al., 2005); these are probably not related to the activity of Hainan plume evidenced by geophysical and geochemical data (e.g., Montelli et al., 2006; Zhao, 2007; Yan and Shi, 2007; Xu et al., 2012), but to the subduction of the paleo-SCS-crust beneath the Borneo. Cullen (2010, 2013) discusses some of the problems with models having extensive late Cenozoic subduction beneath NW Borneo. Due to the scarcity of geochemical data for these calc-alkalic rocks, they are not included in further discussion.

3.2.1. Pre-SCS spreading magmatism (intra-continental rifting)

A large number of Cenozoic volcanics have been reported in a series of Tertiary rifted basins (e.g., the PRMB, the Sanshui Basin, the Lianping Basin, and the Heyuan Basin), which reflect pre-SCS spreading magmatic activities (Table 2, Fig. 3). In these basins, bimodal volcanics were extruded in early Tertiary time. Their eruption ages range from 64 to 43 Ma (K–Ar whole rock dating method) (Zou et al., 1995) or 60–43 Ma (zircon U–Pb dating method) (Zhou et al., 2009) in the Sanshui Basin and from 51.6 to 32 Ma (K–Ar whole rock dating method) (Zou et al., 1995) in the PRMB. The lithology of erupted rocks is relatively complex. For example, in the PRMB there are rhyolite, rhyolitic tuff, dacite tuff, dacite and quartz tholeiite (Table 2).

3.2.2. Syn-SCS spreading magmatism

During Cenozoic seafloor spreading in the SCS, in addition to those producing oceanic crusts at spreading centers of the SCS, igneous activities were relatively weak in most areas of the SCS region. Zou et al. (1995) once reported there existed a few amounts of basaltic activities of this period in the PRMB, and the ages for basaltic rocks have been dated at ~27 (andesite) and 24 Ma (quartz tholeiite) (Table 2, Fig. 3). It need to be noted that IODP leg 349 will possibly obtained the oceanic crust basement of the SCS, which is very important for completely understanding the Cenozoic evolution of the SCS (Li et al., 2013).

3.2.3. Post-SCS spreading magmatism

Intraplate magmatism affected large areas in the Indochina block shortly after the cessation of seafloor spreading., e.g., PRMB, Leiqiong peninsula, Beibu Gulf, Indochina block, Reed Bank and Dangeous Grounds, and SCS basin itself (Fig. 3, Table 2). In addition, the eastward subduction of oceanic crust of the SCS formed during Cenozoic spreading contributed the development of the Luzon island arc.

The eruption of alkali basaltic magma in the PRMB appears to have started at 17.1 Ma (age of alkali basalt determined by K–Ar whole rock dating method) (Zou et al., 1995) when seafloor spreading had almost ceased and subduction of oceanic crust beneath Taiwan was initiated.

In the Leiqiong peninsula, widespread and large volume of mafic volcanics was erupted, including quartz tholeiite and alkali basalt. The ages of volcanism have been dated at 16.7–11.7 Ma and <6.6 Ma (for the quartz tholeiite) and 4–6 Ma and <1 Ma (for the alkali basalt) by K–Ar/Ar–Ar dating method (Zhu and Wang, 1989). In the Beibu Gulf, only alkali basalt has been reported, and its age ranges from 5.4 to 2.7 Ma (K–Ar whole rock dating method) (Jia et al., 2003) to Quaternary (^{14}C dating method) (Li et al., 2005).

Post-spreading gagmatism also occurred in the Khorat Plateau, Dalat, Phuoc Long, Buon Ma Thuot, Pleiku, Xuan Loc, and Ile des Cendres regions in offshore southern Vietnam (Hoang et al., 1996; Zhou and Mukasa, 1997; Hoang and Flower, 1998; Lee et al., 1998; Fig. 3 and Table 2). The ages of volcanism have been dated at 0.9 Ma (K–Ar whole rock dating method) for alkali basalt and hawaiite in the Khorat Plateau (Zhou and Mukasa, 1997), 17.6–7.9 Ma (Ar–Ar whole rock dating method) for quartz tholeiite in the Dalat zone (Hoang and Flower, 1998), <8–3.4 Ma (Ar–Ar whole

Table 2
Data for Cenozoic volcanics from the SCS region. Rock abbreviations: A – andesite; AB – alkali basalt; D – dacite; DT – dacite tuff; H – Hawaiite; OT – olivine tholeiite; QT – quartz tholeiite; R – Rhyolite; RT – rhyolitic tuff.

	Sample number[a]	Sample details		Lithology	Ages (Ma)	Dating method	References
		Depth (m)[b]	Longitude/latitude				
Northern margin of the South China Sea (PRMB, BBG, LQP)							
1	Y21-1-1	1656	Pearl River Mouth Basin	R	51.6	K–Ar(WR)	Zou et al. (1995)
2	L21-1-1	2446.6	(drill cores)	RT	49.33	K–Ar(WR)	
3	L15-1-1	2175		QT	45.1	K–Ar(WR)	
4	L4-1-1	1779.6		DT	43.2	K–Ar(WR)	
5	H21-1-1	4591		D	41.3	K–Ar(WR)	
6	P16-1-1	2389		QT	41.1	K–Ar(WR)	
7	L1-1-1	3454		RT	32 and 33.6	K–Ar(WR)	
8	L11-1-2	1799.6		A	27.2	K–Ar(WR)	
9	X33-2-1A	4883		QT	24.6	K–Ar(WR)	
10	B7-1-1	2429		AB	17.1	K–Ar(WR)	
11	WSH-2		Weizhou island, BBG	AB	5.9	K–Ar(WR)	Jia et al. (2003)
12	SK-1		Sankou Town, BBG	AB	2.4	K–Ar(WR)	
13	W4-1		Weizhou island, BBG	AB	Quaternary	^{14}C	Li et al. (2005)
14			Sanshui Basin	Bimodal volcanisam	60–43	U–Pb(zircon)	Zhou et al. (2009)
15					64–43	K–Ar(WR)	Zhu et al. (1989)
16			Lei–Qiong Peninsula	AB	4–6 Ma and 1 Ma	K–Ar/Ar–Ar	Zhu and Wang (1989)
17				QT	16.7–11.7 Ma and <6.6 Ma	K–Ar/Ar–Ar	
Indochina peninsula (southeastern Vietnam and Thailand)							
18			Khorat Plateau, Thailand,	AB, H	0.9	K–Ar(WR)	Zhou and Mukasa (1997)
19			Dalat	QT	17.6–7.9	Ar–Ar	Lithology data from Hoang et al. (1996); age data from Hoang and Flower (1998)
20			Phuoc Long	QT and OT	<8–3.4	Ar–Ar	
21			Buon Ma Thuot	AB and OT	5.8–1.67	Ar–Ar	
22			Pleiku	OT,AB,QT	4.3–0.8	Ar–Ar	
23			Xuan Loc	OT,AB,basanite	0.88–0.44	Ar–Ar	
24			Ile des Cendres	OT	0.8–0	Ar–Ar	
Southern margin of the South China Sea (Reed Bank, Nansha Is.)							
25	SO23-37	2373	116°36.01′E, 12°5.23′N to 116°36.01′E, 12°05.23′N	Vesicular porphyritic basalt	0.419	K–Ar(WR)	Kudrass et al. (1986)
26	SO23-38	3227–3043	118°18.09′E, 11°44.06′N to 118°18.20′E, 11°44.71′N	Olivine basalt	0.466	K–Ar(WR)	
27	SO23-40	1050 and 765	118°49.00′E, 12°21.38′N and 118°48.42′E, 12°21.53′N	Vesicular basalt	2.7	K–Ar(WR)	
South China Sea Basin (Seamounts)							
28	S04-11	2200	116°05.95′E, 16°20.62′N	AB	7.91 ± 0.19	K–Ar(WR)	Yan et al., 2008b
29	S04-12-10	1290	113°09.56′E, 12°34.32′N	AB	4.78 ± 0.11	K–Ar(WR)	
30	S04-12-11	1290		AB	5.74 ± 0.13	K–Ar(WR)	
31	S04-12-18	1290		AB	5.18 ± 0.17	K–Ar(WR)	
32					6.06 ± 0.29	Ar–Ar	
33	S04-12-20	1290		AB	4.76 ± 0.12	K–Ar(WR)	
34	S04-12-21	1290		AB	4.94 ± 0.11	K–Ar(WR)	
35	S08-69-1	2280	112°32.08′E, 10°19.30′N	AB	3.80 ± 0.10	K–Ar(WR)	
36					4.71 ± 0.34	Ar–Ar	
37	S04-14-1	1470	115°23.07′E, 14°02.35′N	AB	6.33 ± 0.20	K–Ar(WR)	
38					6.64 ± 0.42	Ar–Ar	This study
39	D8	3429	116°59′E, 17°37′N	OT	13.9	K–Ar/Ar–Ar	Wang et al. (1984)
40	D9	3116	116°30′E, 14°48′N	OT and TB	9.9	K–Ar/Ar–Ar	
41	D10	3041	115°35′E, 14°00′N	AB	3.5	K–Ar/Ar–Ar	
Luzon arc at the eastern margin of the SCS							
42			Taiwan Segment	Calc-alkaline arc volcanics	15–1	K–Ar (mainly)	Defant et al. (1989, 1990) and references therein
43			Babuyan Segment		9–Present		
44			Northern Luzon Segment		14–Present		
45			Bataan Segment		7–Present		
46			Mindoro Segment		<2 Ma–Present		

[a] Refers to sample number for land samples; well number for industrial wells or site number for dredged samples.
[b] Refers to absolute depth for granitic rocks in industrial wells, or water depth for dredged samples.

rock dating method) for quartz tholeiite and olivine tholeiite at Phuoc Long (Hoang and Flower, 1998), 5.8–1.67 Ma (Ar–Ar whole rock dating method) for alkali basalt and olivine tholeiite at Buon Ma Thuot (Hoang and Flower, 1998), 4.3–0.8 Ma (Ar–Ar whole rock dating method) for quartz tholeiite, olivine tholeiite and alkali basalt at Pleiku (Hoang and Flower, 1998), 0.88–0.44 Ma (Ar–Ar whole rock dating method) for quartz tholeiite, olivine tholeiite and basanite at Xuan Loc (Ar–Ar dating method, Hoang and Flower, 1998) and 0.8–0 Ma (Ar–Ar whole rock dating method) for olivine tholeiite at Ile des Cendres region (Hoang and Flower, 1998). In general, from ca. 17 Ma to present, the alkalinity of magma gradually increases, from quartz tholeiitic to alkalic magma at ~6 Ma.

Pliocene basaltic rocks have been dredged from Reed Bank and Dangerous Grounds (Kudrass et al., 1986) and dated to be 0.42 Ma

(K–Ar whole rock dating method) for vesicular porphyritic basalt, 0.47 Ma (K–Ar whole rock dating method) for olivine basalt and 2.7 Ma (K–Ar whole rock dating method) for vesicular basalt (Kudrass et al., 1986). Hutchison and Vijayan (2010) reported several single volcanoes in the northwest Palawan trough based on geophysical data, but they have not been sampled and, thus, their ages remain unclear. Recently, Cullen et al. (2013) reported some Pliocene bimodal volcanic rocks with arc-like mantle trace element from the area representing the suture between Luconia and Dangerous Grounds blocks.

The SCS basin is covered by sediments up to ~2 km thick and its igneous basement has not been sampled so far (Shipboard Scientific Party, 2000). Wang et al. (1984), Tu et al. (1992) and Yan et al. (2008a,b) reported some basaltic samples dredged from several seamounts. The K–Ar/Ar–Ar ages reported by Wang et al. (1984) are 13.9 Ma (olivine tholeiite, D8 site), 9.9 Ma (trachybasalt and olivine tholeiite, D9 site) and 3.5 Ma (alkali basalt, D10 site). Yan et al. (2008b) reported that all rock samples from seamounts are alkali basalts and their ages range from 7.9 to 3.8 Ma (Table 2). Yan et al. (2008b) reported that the ages measured using Ar–Ar method are systematically older than those from obtained by the K–Ar method (see also, Baksi, 2003). In general, from 13.9 to 3.5 Ma, the alkalinity of magma appears to increase, and after ~8 Ma, dominantly alkalic magma began to erupt. The compositional evolution of intraplate magmatism in the SCS is similar to that of Indochina block (Hoang et al., 1996; Zhou and Mukasa, 1997) and Leiqiong peninsula (Zhu and Wang, 1989).

In addition, post-spreading volcanism laso occurred in the Luzon arc, and the volcanic arc can be divided into five segments, i.e., Taiwan, Bashi, Northern Luzon, Bataan, and Mindoro (Defant et al., 1989, 1990; Knittel et al., 1995; and references therein). Arc volcanism is caused by the subduction of SCS crust and began at the Taiwan segment shortly after the cessation of seafloor spreading. The Luzon–Taiwan volcanic arc mainly consists of calc-alkaline intermediate to acidic arc volcanic rocks. The ages of the volcanic rocks range from 15 Ma to Recent (Defant et al., 1989, 1990).

In summary, despite the relatively poor quality of some of the age data, available petrologic and geochronologic data for the volcanic rocks in the SCS region allow us to draw the following conclusions. In the beginning, only bimodal volcanism (basaltic rocks and rhyolites) occurred in response to rifting in the northern margin of the proto-SCS. During the Cenozoic seafloor spreading in the SCS, other igneous activities (producing mainly tholeiitic lavas) were relatively weak, and only Zou et al. (1995) reported basaltic activities at ~27 and 24 Ma in the PRMB. Shortly after the cessation of seafloor spreading, convergent calc-alkaline volcanism in response to the subduction of the SCS crust beneath the Philippine Sea plate commenced along the Taiwan–Luzon arc, and this arc volcanism continues at present. Also after the cessation of spreading, widespread volcanic activities occurred in the SCS region, and the nature of these activities temporally evolved from tholeiitic to alkalic.

4. Geochemistry and petrogenesis of late Mesozoic granitoids

In general, compositional data for Mesozoic igneous rocks from the SCS region are scarce, so it is difficult to constrain the petrogenesis of these rocks. For example, there are no reported chemical and isotopic data for granitic rocks from Zhongsha and Xisha micro-blocks (Jin, 1989) and from the Reed Bank and Dangerous Grounds (except for some major element data for rhyolite – Kudrass et al., 1986), only major element data had been reported for Mesozoic rocks from the offshore continental shelf in southern Vietnam (Areshev et al., 1992), and major element plus incomplete trace element or Sr isotope data for Mesozoic rocks from the West Kalimantan (Williams et al., 1988) and the PRMB (Li et al., 1999), respectively. A summary of the chemical data for late Mesozoic granitic rocks from the SCS region are given in Table S1 in the Supplementary materials.

4.1. Major elements

In the TAS (total alkalis ($Na_2O + K_2O$) vs. SiO_2) diagram (Fig. 4), the late Mesozoic samples plot in the calc-alkaline field except for two samples from the PRMB and one sample from the Schwaner Mountains. In the K_2O vs. SiO_2 diagram (Fig. 5), the bulk of the samples plot in the fields of the high-K calc-alkaline and the calc-alkaline rock series, and a small number plot within the field for the shoshonite series (samples from the PRMB and Schwaner Mountains) and low-K tholeiite series (samples from Schwaner Mountains). In the A/NK vs. A/CNK diagram (Al/(Na + K) vs. Al/(Ca + Na + K)) (Fig. 6), most samples plot along the boundary

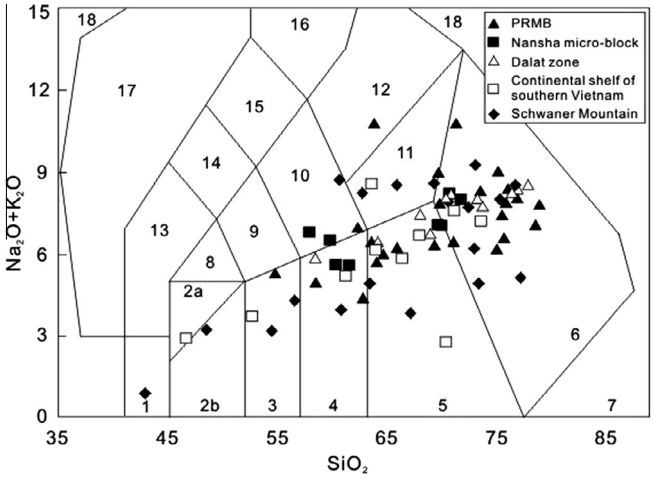

Fig. 4. TAS (SiO_2 vs. $Na_2O + K_2O$) and alkaline discriminantion diagrams for the late Mesozoic granites in the SCS region (Le Maitre, 1989). 1 – peridotite gabbro; 2a – alkaline gabbro; 2b – sub-alkaline gabbro; 3 – gabbro diorite; 4 – diorite; 5 – granodiorite; 6 – granite; 7 – quartzolite; 8 – monzogabbro; 9 – monzodiorite; 10 – monzonite; 11 – Quartz monzonite; 12 – syenite; 13 – feldspathoid gabbro; 14 – feldspathoid monzodiorite; 15 – feldspathoid monzosyenite; 16 – feldspathoid syenite; 17 – feldspathoid pluton; 18 – tavorite/urtite/italite. The dashed line divided igneous rocks into alkalic and tholeiitic series.

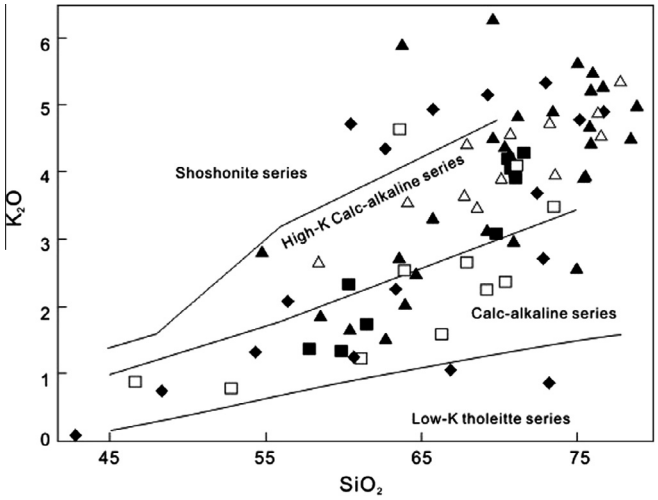

Fig. 5. SiO_2 vs. K_2O for late Mesozoic granites in the SCS region. Symbols and sources of data are as in Fig. 4.

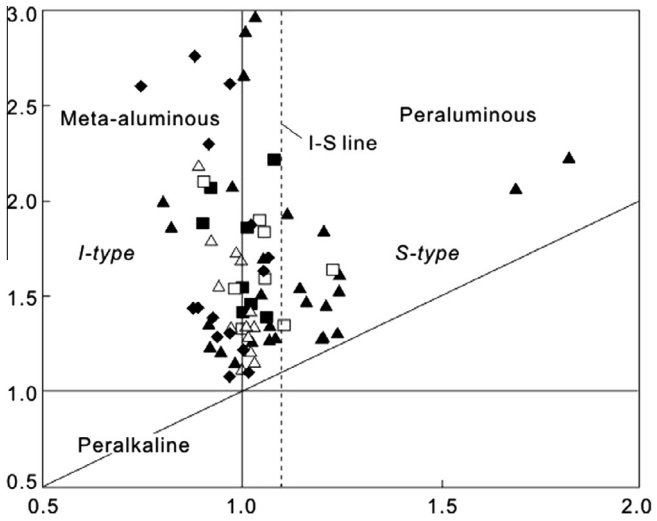

Fig. 6. Shand diagram for late Mesozoic granitic rocks (after Maniar and Piccoli, 1989). The value for the I–S line is from White and Chappell (1983). Symbols and sources of data are as in Fig. 4.

between metaluminous and peraluminous fields and along the I–S boundary defined by White and Chappell (1983), which separates granites derived from igneous (*I*) from those derived from sedimentary (*S*) protoliths. In addition, the Rittman index (σ) values (indicating alkalinity of igneous rock, $\sigma = ((Na_2O\ (wt\%) + K_2O\ (wt\%))/(SiO_2\ (wt\%) - 43))$, of all samples are less than 3. Therefore, the compositional characteristics of the bulk of late Mesozoic granitic rocks suggest that they belong to the I-type calc-alkaline series which may be related to a volcanic arc or a continental arc (Williams et al., 1988; Areshev et al., 1992; Li et al., 1999; Nguyen et al., 2004b; Yan et al., 2010). It must be noted that the A/CNK values of about ten samples (<105 Ma) are more than 1.1, and plot in the right side of I–S line (Fig. 6). This, combined with their high $(^{87}Sr/^{86}Sr)_i$ values for some granites (Table S1), reflects the presence of S-ype granites in the PRMB (Li et al., 1999).

4.2. Trace elements

Average continental crust (Sun and McDonough, 1989)-normalized trace element concentration diagrams are shown in Fig. 7. Most intermediate to acidic granitic rocks from the Nansha micro-block (Yan et al., 2010) show weak negative Eu (Fig. 8a), Nb,

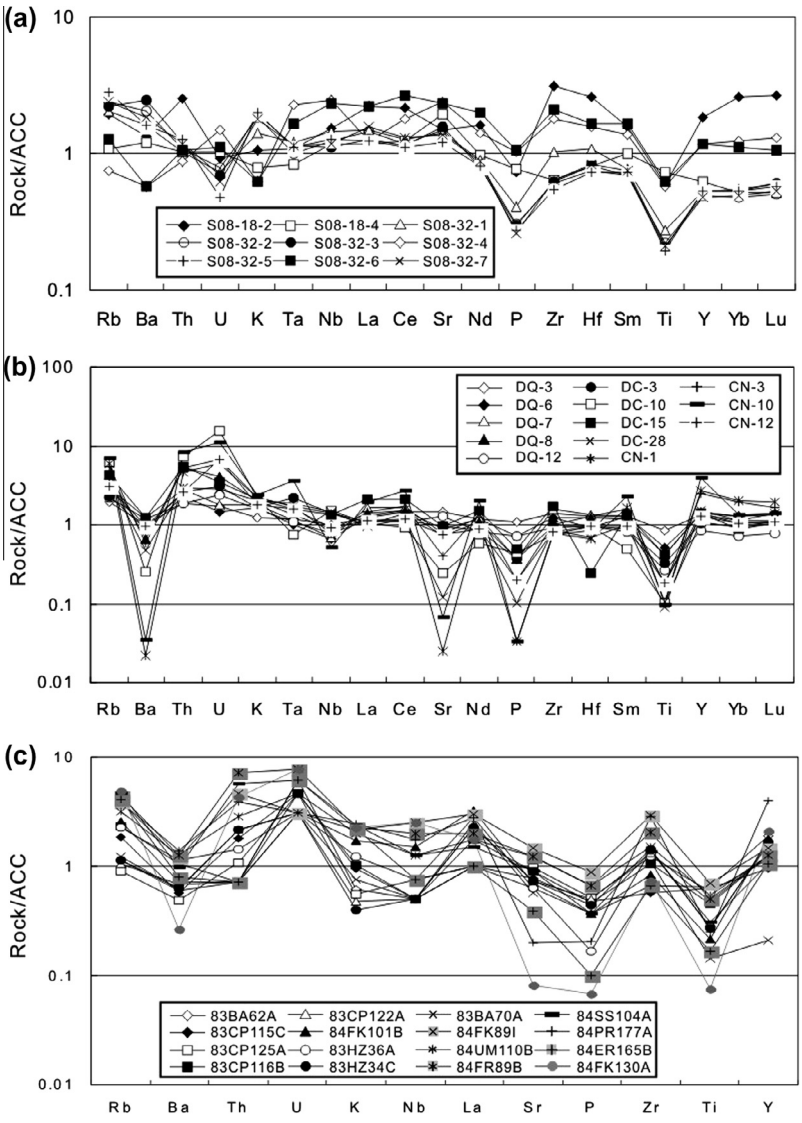

Fig. 7. Average continental crust-normalized trace element concentration diagrams for the late Mesozoic granitic rocks from the SCS region. Trace element abundances of average continental crust (ACC) are from Rudnick and Gao (2003). (a), Nansha micro-block; (b) Dalat zone in the southern Vietnam; (c) Schwaner Mountains. Note that some of the samples that have negative Sr- and P-anomalies also have negative Ba and/or Ti anomalies.

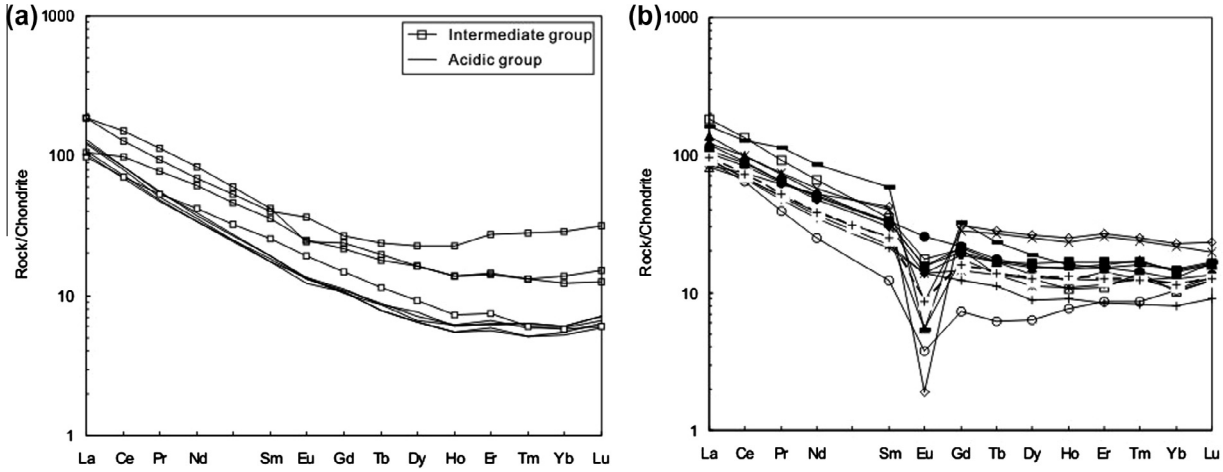

Fig. 8. C1 chondrite-normalized REE abundances patterns for the Cenozoic volcanics from the SCS region. C1 chondrite REE abundances are from Sun and McDonough (1989). (a), Nansha micro-block; (b) Dalat zone in the southern Vietnam.

Ta, P and Ti anomalies and weak positive radiogenic element (e.g., Th, U and K) anomalies (Fig. 7a), which may reflect arc tectonic signature, source characteristics or effects of magmatic differentiation. However, for several samples, the fractionation of Nb–Ta from Zr–Hf, indicated by Nb–Ta trough and Zr–Hf peak (Fig. 7a), may have been also due to the addition of low-Mg-number amphiboles from unmodified mantle into parental magmas of some granitic rocks (e.g., Tiepolo et al., 2001). The three granitic suites from southern Vietnam studied by Nguyen et al. (2004b) (Fig. 7b) all show strong negative Ba, P, Sr and high field strength elements (HFSE; e.g., Nb, Ta, and Ti) anomalies and positive Th, U and K anomalies. The characteristic trace elements features of granitic rocks from the Schwaner Mountains in west Kalimantan (Williams et al., 1988) are similar to those from southern Vietnam (Fig. 7c), which may indicate a common petrogenesis.

Chondrite-normalized rare earth element (REE) patterns are shown in Fig. 8. Granitic rocks from the Nansha micro-block (Yan et al., 2010) have variable $(La/Yb)_N$ ratios (e.g., 6.1–16.2 for acidic rocks and 16.6–22.8 for intermediate rocks – Table S1), but have broadly similar REE distribution patterns (Fig. 8a). The three volcanic suites from southern Vietnam also show similar distribution patterns (Nguyen et al., 2004b, Fig. 8b) as well as fairly similar $(La/Yb)_N$ ratios (3.6–11.0 for Cana suite, 6.3–18.0 for Deoca suite, and 7.6–24.0 for Dinhquan suite – Table S1). The high $(La/Yb)_N$ (>1 for all samples) ratios and negative Eu anomalies of granitic rocks from the PRMB indicate that they have experienced strong fractional crystallization (e.g., plagioclase) (Li et al., 1999).

4.3. Sr, Nd and Pb isotopes

Strontium, Nd and Pb isotopic data are shown in Figs. 9 and 10. Fig. 9 shows several mixing curves between a constant mantle end-member and upper crust, lower crust, bulk crust, or sample S08-18-2 from the Nansha micro-block. This figure simply illustrates that late Mesozoic granitic rocks from the SCS region could be produced through contamination of mantle-derived magmas during their ascent with various types of crustal-derived materials.

The granitic rocks from the Nansha micro-block, similar to those from Nanling–Hainan block (Zhang et al., 1994), have more radiogenic Pb isotopic ratios ($(^{206}Pb/^{204}Pb)t$ = 18.60–18.76 with an average value of 18.69, $(^{207}Pb/^{204}Pb)t$ = 15.64–15.71 with an average value of 15.67, $(^{208}Pb/^{204}Pb)t$ = 38.50–38.89 with an average value of 38.73) (Yan et al., 2008a) than those from southern Vietnam ($(^{206}Pb/^{204}Pb)t$ = 18.45–18.57 with an average value of 18.49, $(^{207}Pb/^{204}Pb)$ t = 15.53–15.55 with an average value of 15.54, $(^{208}Pb/^{204}Pb)t$ = 38.31–38.45 with an average value of 38.36) (Nguyen et al., 2004a) (Table S1). These clearly indicate that the source composition/evolution of the Nansha micro-block is different from that of the Dalat zone in southern Vietnam, which belongs to the Indochina block. In Fig. 10, samples from the Nansha micro-block plot within the field of the Nanling–Hainan block whereas samples from the Dalat zone in southern Vietnam plot away from the field of the Nanling–Hainan block.

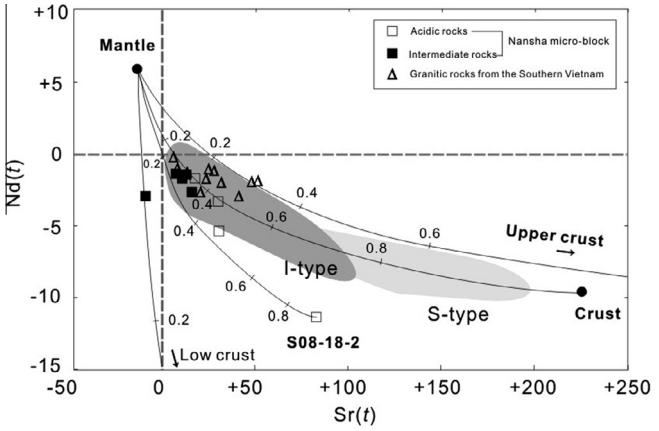

Fig. 9. $\varepsilon Sr(t)$ vs. $\varepsilon Nd(t)$ plot for late Mesozoic granitic rocks from the SCS region (after McCulloch and Chappell, 1982). Crustal component (A): $\varepsilon Nd = -9$, Nd = 28 ppm, $\varepsilon Sr = 227.2$, Sr = 140 ppm; Mantle component (B): $\varepsilon Nd = +6$, Nd = 14 ppm, $\varepsilon Sr = -14.2$, Sr = 470 ppm. Data for Sr and Nd of upper crust, lower crust, total crust, and mantle are from Faure (1986).

4.4. Petrogenesis

4.4.1. PRMB

Based on petrological, geochronological and geochemical data, late Mesozoic granitic rocks from PRMB includes an early (>105 Ma) stage of I-type granites (ACNK < 1.1 and $(^{87}Sr/^{86}Sr)_i < 0.710$) and a later stage (<105 Ma) of S-type granites (ACNK > 1.1 and $(^{87}Sr/^{86}Sr)_i > 0.710$) (Li et al., 1999). The geochemical characterisitcs of I-type granites in PRMB is similar to those from the Nansha block (Yan et al., 2010), which implies that both of them may have experienced similar magmatic processes. Both types experienced extensive fractional crystallization. Due to the

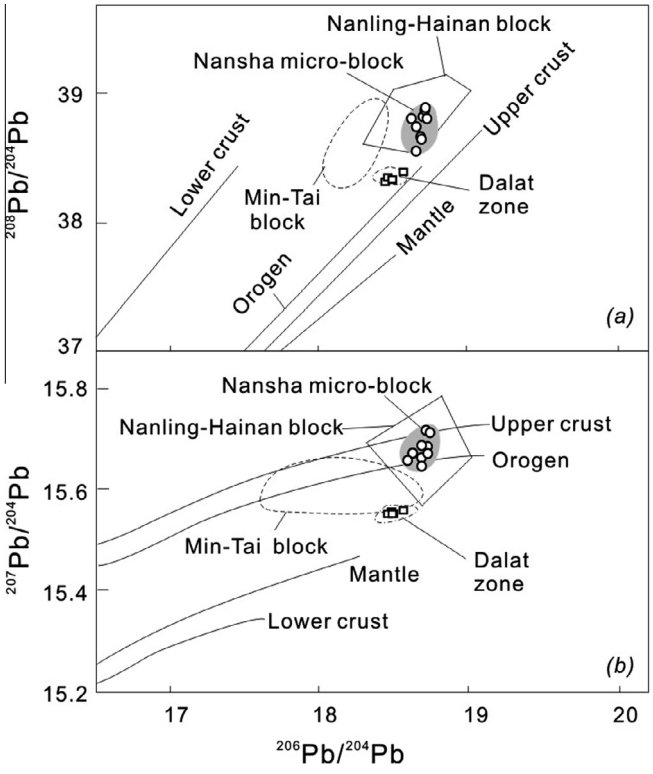

Fig. 10. $^{206}Pb/^{204}Pb$ vs. $^{207}Pb/^{204}Pb$ and $^{208}Pb/^{204}Pb$ plots of late Mesozoic granitic rocks from the SCS region (after Zartman and Haines, 1988).

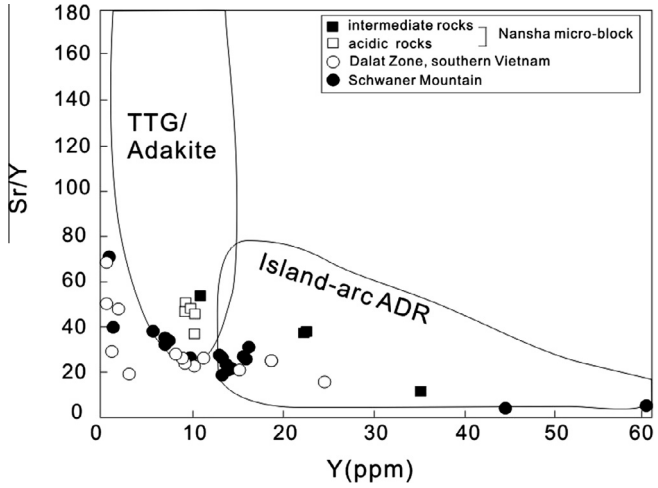

Fig. 11. Sr/Y–Y variation diagram for late Mesozoic granites from the SCS region (after Martin, 1995, 1999). TTG: tonalite–trondhjemite–granodiorite; ADR: andesite–dacite–rhyolite.

scarcity of Nd isotopic data, however, their detailed petrogeneses cannot be further constrained. However, the available data are in accord with the evolutionary trend of a typical orogenic setting (Hawkesworth and Kemp, 2006) where an earlier volcanic arc, dominated by I-types granite, is usually followed by a later syn-collisional setting, dominated by S-type granite.

4.4.2. Nansha micro-block

The A/CNK values (<1.1, Fig. 6), trace element characteristics (e.g., negative HFSE anomalies - Fig. 7a) and isotopic ratios ($(^{87}Sr/^{86}Sr)_i < 0.710$ for most samples, Fig. 9) of granitic rocks from the Nansha micro-block suggest that they are also I-type, similar to some granitic rocks from Taiwan (Lan et al., 1996). They are mainly crustal-derived with variable contributions from mantle-derived magmas, since they have low, variable initial Sr values and variable, negative $\varepsilon Nd(t)$ values (Yan et al., 2010). Furthermore, samples do not show any obvious Eu anomalies, suggesting that they were derived from partial melting of a source which did not contain plagioclase as residue. However, intermediate rocks could have come from partial melting of mixed sources and acidic rocks may have originated from partial melting of thickened mafic crust with garnet in the residue (Yan et al., 2010) on the basis of their Sr/Y–Y variation (after Martin, 1995) (Fig. 11).

Fractional crystallization during the formation of Nansha micro-block granitic rocks is suggested by their depletions in HFSE (Fig. 7a) and similar REE distribution patterns (Fig. 8a). Negative Ti anomalies are generally associated with fractionation of Ti-bearing phases and negative P anomalies result from apatite separation. In general, the fractionation effect is greater in the light REE than in the heavy REE for the older intermediate rocks than in the later acidic rocks.

Petrogenesis models for granitic rocks from the Nansha micro-block had been proposed by Yan et al. (2010). These granites can be divided two groups. Group I (i.e., intermediate rocks) (Fig. 9) are produced by partial melting of older Precambrian basement, which may have existed in all micro-blocks dispersed in the SCS (Jin, 1989; Liu et al., 2002, 2006; Yan et al., 2008c and T_{DM} age in Table S1), with the variable influence of mantle-derived magma which results from the interaction of released fluids from the subducted slab and the overlying mantle wedge in a general convergent margin setting. The suggestion that subduction components affected on its petrogenesis is consistent with the notion that there was an Andean-type continental margin in the SCS region during the Mesozoic era (Holloway, 1982; Taylor and Hayes, 1980, 1983). Group II (acidic rocks) (Fig. 9) result from partial melting of lower crustal basic rocks (amphibolite) (Muir et al., 1995) and/or further partial melting of the Group I rocks associated with the variable influence from the underplating mantle-derived magma resulting from lithospheric extensional regime widely occurring in east China in the late Mesozoic era (Wu et al., 2005). This evolution model basically follows the common trend of continental crust evolution (Hawkesworth and Kemp, 2006).

4.4.3. Southern Vietnam

A/CNK values (Fig. 6), trace element characteristics (negative HFSE anomalies, Fig. 7b) and isotopic characteristics ($(^{87}Sr/^{86}Sr)_i < 0.707$ for most samples, Table S1 and Fig. 9) of granitic rocks from the southern Vietnam suggest that they also are of I-type granites and, thus, similar to those in the Nansha micro-block (Yan et al., 2010) and some granitic rocks from Taiwan (Lan et al., 1996).

Based on geochemical and experimental data, Nguyen et al. (2004b) suggested that the voluminous felsic magmas in southern Vietnam could have not been generated by magmatic differentiation or AFC processes of mantle-derived mafic magmas. Instead they proposed a petrogenetic model that is similar to that for the Nansha micro-block. The protolith of granitic rocks in southern Vietnam may be the compositionally heterogeneous Precambrian Kontum massif that is present in the lower crust (Nam et al., 2001; Lan et al., 2003; Nguyen et al., 2004b). The underplating of mantle-derived basaltic magma produced during the late Mesozoic subduction process provided the heat for the partial melting of the lower crust. Variable addition of juvenile mantle-derived magma to the partial melts from the lower crust can well account for the decrease in the initial $(^{87}Sr/^{86}Sr)_i$ ratios from the common values of the lower crust (possibly represented by sample CN-1 ($(^{87}Sr/^{86}Sr)_i = 0.741$), to 0.705–0.707 (Table S1). This also resulted

in the decrease of the TDM values from 1.2–2.4 Ga of Kontum massif (Lan et al., 2003) or 1.65 Ga represented by sample CN-1 to 0.8–1.16 Ga (Table S1). Finally, the mixed magma experienced different extents of fractional crystallization during its ascent, e.g., fractionation of K-feldspar and plagioclase in the Deoca rock suite, fractionation of sphene, apatite, zircon, allanite and titanite in the Dinhquan rock suite, and fractionation of hornblende and/or titanite in the Deoca rock suite (Nguyen et al., 2004b).

4.4.4. Other regions

Only major element compositions are available for granitic rocks from the continental shelf of offshore southern Vietnam (Areshev et al., 1992) and the Schwaner Mountains in west Kalimantan (Williams et al., 1988). So, it is not possible to further constrain their petrogeneses in detail. Due to the close temporal and spatial relationship of granitic rocks from the continental shelf offshore southern Vietnam to those from southern Vietnam, we infer that they have similar petrogenesis. On the other hand, based on their major element compositions and Williams et al. (1988)'s simple plate reconstruction, the petrogenesis of late Mesozoic granitic rocks in the Schwaner Mountains may be arc-related (Hamilton, 1979).

5. Geochemistry and petrogenesis of Cenozoic igneous rocks

Chemical analyses of Cenozoic igneous rocks from the SCS and surrounding region are given in Table S2 in the Supplement materials. Note that data from the Lianping, Heyuan and Sanshui basins in Guangdong province, which are tectonically related to the PRMB, are included in Table S2 and in the discussion below.

5.1. Major elements

5.1.1. PRMB

In the TAS diagram (Fig. 12), the older volcanic rocks (>17 Ma) plot in the field for the calc-alkaline rock series, and show distinct bimodal (acidic and basic) distribution patterns. Later volcanics (<17 Ma) are basaltic rocks and plot within the alkali series. The changes of major element characteristics from >17 Ma calc-alkaline rocks to <17 Ma alkali rocks, may reflect that with decreasing age, the depth of magma source gradually increases (Zou et al., 1995). This not only reflects changes in extensional extent in the whole extensional lithospheric setting, but changes in the deep geodynamic setting as well. For example, >17 Ma calc-alkaline rocks may reflect the PRMB is a continental rifted basins lying at the wholly rifted, northern margin of the SCS, and <17 Ma alkali rocks may reflect a the deep geodynamic setting of PRMB is mantle plume.

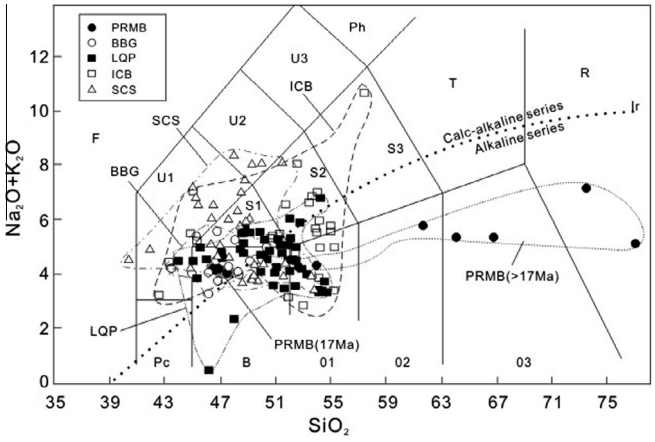

Fig. 12. TAS (SiO_2 vs. $Na_2O + K_2O$) and alkaline discrimination diagrams for Cenozoic volcanics in the SCS region (Le Maitre, 1989). Pc – oceanite; B – basalt; O1 – basaltic andesite; O2 – andesite; O3 – dacite; R – rhyolite; S1 – trachybasalt; S2 – basaltic trachyandesite; S3 – trachyandesite; T – trachyte-trachydacite; F – feldspathoidite; U1 – tephrite–basanite; U2 – phonolitic tephrite; U3 – tephritic phonolite; Ph – phonolite; Ir – Irvine line dividing alkalic and tholeiitic series (after Irvine and Baragar, 1971). PRMB – Pearl River Mouth Basin; BBG – Beibu gulf; LQP – Leiqiong peninsula; ICB – Indochina block; SCS – South China Sea.

5.1.2. Beibu Gulf (BBG)

In the TAS diagram (Fig. 12), all volcanic rocks including Middle Pleistocene, Late Pleistocene and Holocene volcanics from this area are basaltic and plot within the field for alkali rock series, and these are consistent with their high Rittmann index values, ranging from 3.0 to 13.0. However, the relationship between MgO and other oxide contents is not clear when all voclanics plotted in the same figure, and the authors suggested that the magmatic evolution for Late Pleistocene volcanic rocks from this area is controlled by plagioclase and olivine fractionation (Li et al., 2005).

5.1.3. Leiqiong peninsula

In the TAS diagram (Fig. 12), all volcanic rocks from this area are basaltic and plot both within the fields of alkali and sub-alkalic rock series. There is a great degree of overlap in the compositions of the older (>6 Ma), which are mainly sub-alkaline (i.e., tholeiitic) lavas (Zhu and Wang, 1989) and the younger (<6 Ma to recent) alkalic and tholeiitic lavas; they were also erupted together (Zhu and Wang, 1989; Flower et al., 1992; Zou and Fan, 2010). As a whole, the major element compositions of volcanics in this area are transitional between mid-ocean ridge basalt (MORB) and ocean island basalt (OIB), and they may have been produced by continental intraplate magmatism and/or continental margin calc-alkaline magmatism (Zhu and Wang, 1989).

5.1.4. Indochina block

In the TAS diagram (Fig. 12), the Cenozoic basalts from Vietnam plot within the field of alkali and sub-alkali rock series and the young (0.9 Ma) basalts from Khorat (Thailand) plot within the alkali series only. Each basalt center in Vietnam is characterized by up-section increases in the proportion of SiO_2-undersaturated flows, overall Mg-number, and CaO/Al_2O_3 ratios; and these reflect variation in mantle source composition and fractional crystallization (Hoang and Flower, 1998). Based on major element data, Hoang et al. (1996) suggested that a sharp secular change from more- to less-refractory sources occurred at most basalt centers. The Khorat basalts can be subdivided into two groups; group I that shows a good correlation between $Na_2O + K_2O$ and other oxides which implying some fractional crystallization, chiefly of olivine, and group II that shows no correlation suggesting no obvious fractional crystallization occurring during magmatic evolution (Zhou and Mukasa, 1997).

5.1.5. South China Sea Basin

In the TAS diagram (Fig. 12), all volcanic rocks from this area are basaltic and plot within both fields of alkalic and sub-alkalic rock series. However, older (>8 Ma) basalts tend to be mainly sub-alkalic (tholeiitic) whereas the younger (<8–0.5 Ma) basalts are predominantly alkalic (Tu et al., 1992; Yan et al., 2008a,b,c). In the younger alkali basalts, major and trace element correlations with MgO contents basically follow the typical OL + CPX fractional crystallization and/or phenocryst accumulation trends (Yan et al., 2008a,b,c).

5.2. Trace elements

Primitive mantle-normalized trace element spidergrams and chondrite-normalized REE distribution patterns are shown in Figs. 13 and 14, respectively.

5.2.1. PRMB

In Fig. 13a, most of the older (>17 Ma) basaltic and acidic volcanics show similar trace element characteristics, i.e., enrichment in large ion lithophile element (LILE) and depletion in HFSE, similar to typical island arc basalt (IAB). The depletion of HFSE for the older (>17 Ma) volcanics in PRMB may reflect that parent magma from the mantle source has been influenced by continental crust (with marked HFSE depletion)-wall rock contamination during its ascent to the surface. Younger volcanics (<17 Ma) are enriched in both LILE and HFSE, similar to typical OIB (Sun and McDonough, 1989) and basalts from the seamounts in the SCS (Yan et al., 2008a). This geochemical characteristics for younger (<17 Ma) volcanics may reflect that after 17 Ma, the PRMB was in an intraplate setting, as inferred by major element geochemistry. In Fig. 14a, the younger volcanics show higher LREE/HREE enrichment than the older volcanic rocks, with $(La/Yb)_N$ = 16.5 for younger volcanics vs. 7.7 for the older volcanics (Table S2), which reflects that the extent of partial melting of mantle source for younger volcanics is lower than that for older volcanics. There is no Eu anomaly in either rock groups.

5.2.2. Beibu Gulf (BBG)

Several samples show Th and U depletion, but all samples show enrichment in LILE and HFSE (Fig. 13b), similar to typical OIB (Sun and McDonough, 1989). All samples show high LREE/HREE ratios, with $(La/Yb)_N$ = 11.9–27.0, again similar to typical OIB (Fig. 14b; Table S2). There is no Eu anomaly in these rocks.

5.2.3. Leiqiong peninsula

Zhu and Wang (1989) did not provide the trace element data for the older volcanics (16.7 to 11.7 Ma), so there is little information

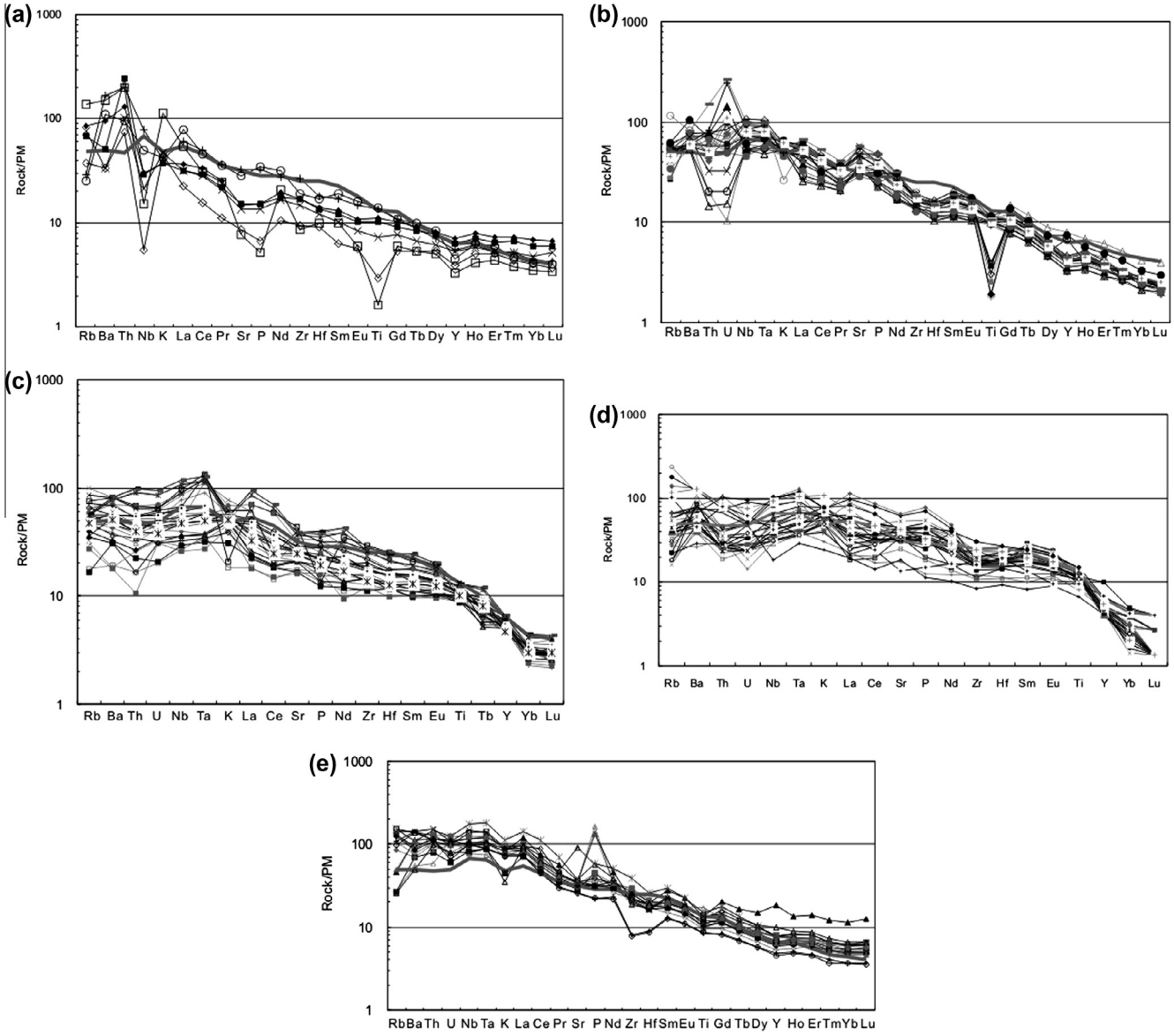

Fig. 13. Primitive mantle-normalized trace element concentration diagrams for Cenozoic volcanics from the SCS region. Trace element abundances of the primitive mantle (PM) and OIB are from Sun and McDonough (1989). (a) Pearl River Mouth Basin (PRMB); (b) Beibu Gulf (BBG); (c) Leiqiong Peninsula; (d) Indochina Block; (e) South China Sea. The distribution pattern for OIB (grey bold line) is shown for reference.

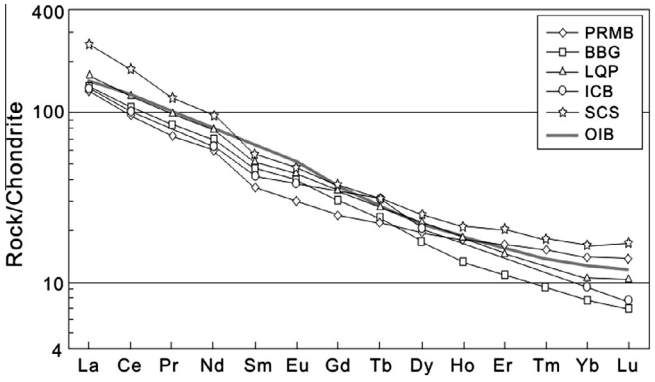

Fig. 14. C1 chondrite-normalized REE abundances patterns for the Cenozoic volcanics from the SCS region. C1 chondrite REE abundances and OIB data are from Sun and McDonough (1989). The figure shows average REE values for samples from Pearl River Mouth Basin (PRMB), Beibu Gulf (BBG), Leiqiong Peninsula (LQP), Indochina Block (ICB) and South China Sea (SCS). The distribution pattern for OIB (grey bold line) is shown for reference.

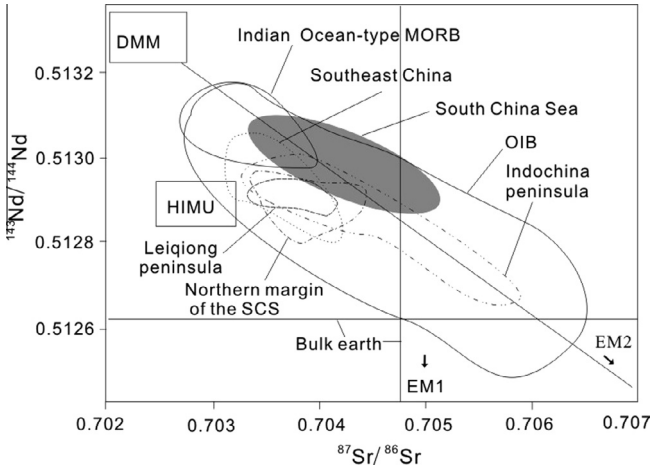

Fig. 15. $^{143}Nd/^{144}Nd$ vs. $^{87}Sr/^{86}Sr$ diagram for the Cenozoic volcanics from the SCS region. Approximate fields for the proposed DMM, HIMU, EM1 and EM2 mantle endmembers are from Zindler and Hart (1986). The field for OIB is from Staudigel et al. (1984); the field for Indian Ocean-type MORB is from Mahoney et al. (1989). Data sources: Leiqiong Peninsula from Zhu and Wang (1989), Tu et al. (1991) and Zou and Fan (2010); Indochina from Hoang et al. (1996) and Zhou and Mukasa (1997); Northern margin of SCS from Zou et al. (1995) and Li et al. (2005); Southeast China from Chung (1999) and Zou et al. (2000); Seamounts in SCS from Tu et al. (1992) and Yan et al. (2008a).

to accurately constrain their petrogenesis. Most of the younger samples (<6.6 Ma) show enrichment in LILE and HFSE (Fig. 13c), similar to those of BBG and typical OIB (Fig. 13b). The younger samples also show high light REE/heavy REE ratios, with $(La/Yb)_N$ = 5.8–21.7 (Table S2), again similar to typical OIB. There is a general increase in light REE/heavy REE ratios from tholeiitic to alkalic basalts. There is no Eu anomaly in these rocks (Table S2).

5.2.4. Indochina block

All Indochina block samples generally show enrichment in LILE and HFSE (Fig. 13d), similar to those from BBG (Fig. 13b) and Leiqiong (Fig. 13c), which are similar to typical OIB. All samples show variable enrichment in LREE/HREE ratios, with $(La/Yb)_N$ = 4.8–59.9 for Vietnam basalts and 3.5–35.1 for Khorat basalts (Fig. 14d; Table S2). No negative Eu anomalies are observed.

5.2.5. South China Sea Basin

As a whole, available SCS basin samples are enriched in LILE and HFSE and depleted in Yb, Sc and Sr (Fig. 13e) and, thus, are different from MORB and IAB, but similar to intraplate OIB (Sun and McDonough, 1989; Niu and O'Hara, 2003). It is noteworthy that the Ce/Pb and Nb/U ratios of these SCS basin basaltic rocks (Yan et al., 2008a,b,c) are close to those for primitive mantle (Hofmann, 1988, 1997), and are obviously higher than the average values for the upper crust (Taylor and McLennan, 1985). Except for two tholeiitic rock samples showing light REE-depleted characteristics (Tu et al., 1992), all other samples from the SCS show strong enrichment of light REE (Fig. 14), with $(La/Yb)_N$ = 10.3–23.9 (Table S2), suggesting that the extent of partial melting of the mantle source is relatively low. No negative Eu anomaly is observed, indicating that plagioclase fractionation was not significant during the generation and evolution of these magmas (Yan et al., 2008a,b,c).

5.3. Sr–Nd–Pb isotopes

Strontium, Nd and Pb isotopic data are summarized graphically in Figs. 15 and 16, and data for Cenozoic basalts from southeast China (Chung, 1999; Zou et al., 2000) are plotted for comparison.

5.3.1. PRMB

Of the two basaltic rocks analyzed, the older one ($(^{87}Sr/^{86}Sr)_i$ = 0.70569, $(^{143}Nd/^{144}Nd)_i$ = 0.51254) is more enriched than the younger one ($(^{87}Sr/^{86}Sr)_i$ = 0.70396, $(^{143}Nd/^{144}Nd)_i$ = 0.51289). The combined Sr, Nd and Pb data plot within the field for the northern margin of the SCS (Figs. 15 and 16).

5.3.2. Beibu Gulf (BBG)

The BBG basalts, from the northern margin of the SCS, plot within the field for OIB (Figs. 15 and 16). The variations in their isotopic ratios ($(^{87}Sr/^{86}Sr)_i$ = 0.70352–0.70443; $(^{143}Nd/^{144}Nd)_i$ = 0.51280–0.51291) reflect a moderately heterogeneous, asthenospheric source (Fig. 15). However, their Pb isotopic ratios show large variations (Fig 16; Table S2), reflecting a more heterogeneous source. All Pb isotope data plot above the northern hemisphere reference line (NHRL) (Hart, 1984), between depleted MORB mantle (DMM) and enriched mantle 2 (EM2 – Fig. 16).

5.3.3. Leiqiong peninsula

Although there are some differences in the Sr and Nd isotopic compositions of the alkalic series and sub-alkalic basalts (Table S2), which may reflect heterogeneity in their mantle source, all samples from this area plot within the field for the northern margin of the SCS (Fig. 15). As a whole, all samples are characterized by highly radiogenic Pb isotopic ratios. All samples plot above the NHRL and within the field of the Dupal isotopic anomaly (Hart, 1984; Castillo, 1988) (Fig. 16; Tu et al., 1991; Zou and Fan, 2010).

5.3.4. Indochina block

The Sr and Nd isotopic compositions of Vietnamese basalts are more variable than those of Khorat basalts (Table S2 in Supplement materials), suggesting that the mantle source of the former is more heterogeneous than that of the latter. The field for all samples from this area is similar to that of the whole northern margin of the SCS, forming an elongated field which lies on a line connecting DMM and EM2. All samples from the Indochina block also plot above and subparallel to the NHRL (Fig. 16) and, thus, the Pb isotopic compositions of most Cenozoic basalts from Indochina block exhibit the characteristics of the Dupal isotopic anomaly, similar to those from the northern margin of the SCS (e.g., Tu et al., 1991; Zou and Fan, 2010) and other western Pacific marginal basin (e.g., Hickey-Vargas et al., 1995; Castillo, 1996).

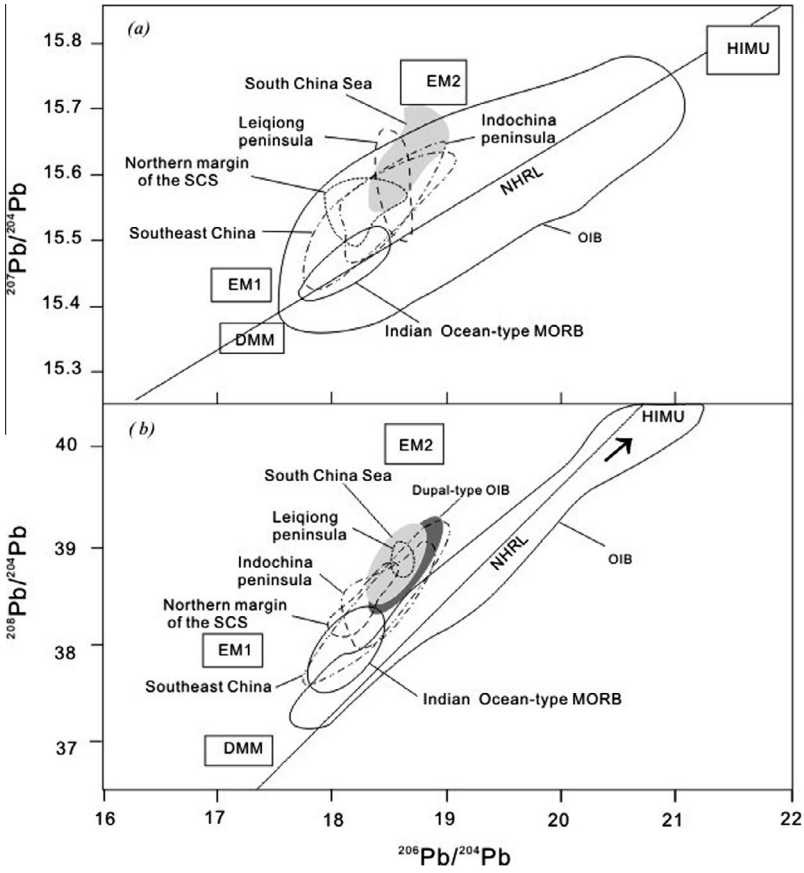

Fig. 16. $^{207}Pb/^{206}Pb$, $^{208}Pb/^{206}Pb$ vs. $^{206}Pb/^{204}Pb$ diagram for the Cenozoic volcanics from the SCS region. Sources of data for the DMM, HIMU, EM1, EM2 and Indian Ocean-type MORB fields are the same as in Fig. 15. NHRL is North Hemisphere reference line (Hamelin and Allègre, 1985). The field for Dupal anomaly is from Hart (1984).

5.3.5. South China Sea Basin

Most of the SCS basin samples plot in the OIB field (Fig. 15), overlapping with basaltic rocks from the Leiqiong peninsula (Tu et al., 1991; Zou and Fan, 2010), northern margin of the SCS (Zou et al., 1995; Li et al., 2005), Indochina block (Hoang et al., 1996; Zhou and Mukasa, 1997), and southeast China (e.g., Zou et al., 2000). Fig. 15 shows a simple binary mixing trend between EM2 and a moderately depleted Indian Ocean MORB-like basalts or DMM component (Yan et al., 2008a). In present study, EM2 represents an undepleted asthenospheric mantle influenced by the Hainan mantle plume (more discussion below), and the DMM is the depleted lithospheric mantle resulting from a previous extraction event. In Pb–Pb isotopic plots (Fig. 16), all samples again lie above the NHRL, having higher $^{207}Pb/^{204}Pb$ and $^{208}Pb/^{204}Pb$ at a given $^{206}Pb/^{204}Pb$ ratio, extending towards the EM2 component. The SCS lavas thus exhibit the characteristics of the Dupal anomaly (Hart, 1984; Castillo, 1988), the origin of which in the SCS is still a matter of debate (e.g., Tu et al., 1992; Castillo, 1996; Yan et al., 2008a).

5.4. Petrogenesis

5.4.1. PRMB

The PRMB, together with Sanshui, Lianping and Heyuan basins in Guangdong province, China, have been regarded as contemporaneous and co-genetic Tertiary rifted basins at the northern margin of the SCS and, thus. the petrogeneses of their igneous basements should be the same. Chung et al. (1997) proposed a "double-diffusive" magma chamber model to account for the formation of the bimodal suites of volcanic rocks in Sanshui, Lianping and Heyuan basins. Zhou et al. (2009) further proposed that both the basaltic and rhyolitic magmatic suites were derived from a similar enriched mantle by low degree partial melting, but experienced different magma chamber processes (e.g., wall rock contamination or fractional crystallization). Based on their similar tectonic setting and presence of bimodal volcanism (>17 Ma) in the PRMB and in several basins in Guangdong province, we prefer to adopt the above model of Zhou et al. (2009) for the petrogenesis of the older (>17 Ma) PRMB volcanic rocks. On the other hand, the source of the younger (<17 Ma) volcanic rocks in the PRMB is an enriched mantle plume, and the dominantly alkalic magmas were produced by low degree partial melting at deeper level in the mantle of such a source due to increasing extent of rifting in the PRMB (Zhou et al., 2009). During its ascent to the surface, the alkalic magmas were not significantly modified by differentiation processes other than fractional crystallization. The evolution of the PRMB follows the general evolutionary history of rifted basins wherein the nature of their magmatic evolution is a general response to the evolution of the rifting process (Zou et al., 1995; Roy, 2001).

5.4.2. Beibu Gulf (BBG)

Jia et al. (2003) proposed that the parental magma of the relatively older (5.9–2.4 Ma) basalts in the BBG area was derived from partial melting of a primitive mantle, based on their trace element geochemical characteristics, i.e., its Nb/Ta = 17.75 (average) and Zr/Hf = 39.87 (average) (Table S2) are close to those of primitive mantle (17.5 and 36.27, respectively) and obviously higher than those continental crust (12 and 11, respectively) (Sun and McDonough, 1989). These basalts are strongly enriched in light

REE (Fig. 14b) and LILE (Fig. 13b), suggesting that they may have been produced by a low degree partial melting of such mantle.

The Quaternary basaltic rocks in Weizhou island in the BBG were most probably derived from the same primitive mantle source, but have systematically higher Mg number than the older volcanic rocks (Li et al., 2005). Geochemical data indicate that the older volcanic rocks evolved from a primary magma by fractional crystallization of olivine and plagioclase, whereas the younger ones represent an almost unmodified primary magma. Trace element characteristics (Fig. 13b, Fig. 14b and Table S2) of BBG basalts are close to that of a primitive mantle, which suggests that their parental magmas did not undergo crustal contamination during their ascent to the surface.

5.4.3. Leiqiong Peninsula

The mantle source of the older (>6 Ma) volcanics in this area have transitional characteristics between MORB and OIB (Fig. 12 and Table S2; Zhu and Wang, 1989). Due to the scarcity of trace element data, the petrogenesis of the volcanics cannot be further discussed.

Tu et al. (1991) and Flower et al. (1992) proposed that the source of the younger (<6 Ma, especially the Quaternary) volcanic rocks is the lower lithosphere consisting of underplated asthenospheric melt overprinted by radiogenic melts of previously subducted sediments. Based on newly acquired Sr–Nd–Pb and U–Th isotopic data, Zou and Fan (2010) recently proposed that the EM2 mantle source for the Quaternary Hainan basalts is in the mantle transition zone or, more likely, lower mantle. The excess mantle potential temperatures beneath Hainan island, calculated from the geochemistry of its late Cenozoic basalts, also support the existence of a mantle plume beneath the island (Wang et al., 2012). The above conclusions and/or inferences are consistent with the recognition of the Hainan plume by geophysical means (e.g., Lebedev et al., 2000; Lebedev and Nolet, 2003; Montelli et al., 2006; Zhao, 2007). Trace element and REE characteristics (Fig. 13c and Fig. 14c) reflect that Quaternary Hainan basalts can be produced by low degree partial melting of EM2 and DMM sources (Figs. 15 and 16). During their ascent to the surface, parental magmas of these volcanics were not significantly modified by crustal contamination because their trace element geochemical characteristics, i.e., their Nb/Ta = 15.25 (average) and Zr/Hf = 41.49 (average) (Table S2) are close to those of primitive mantle and obviously higher than those continental crust (Sun and McDonough, 1989), although shallow-level fractional crystallization played an important role for modifying primary compositions.

5.4.4. Indochina

Hoang et al. (1996) and Hoang and Flower (1998) suggested that there were two eruptive episodes for most of the volcanic centers in Vietnam. An older series (olivine tholeiites) and a younger series (olivine tholeiites, alkali basalts, and basanites) were formed by large melt fractions from a refractory, lithospheric mantle and by smaller melt fractions from a more fertile, asthenospheric mantle, respectively, to form these centers. Alternatively, the lavas erupted at the centers all came from a mantle plume with EM2 characteristics, based on Sr–Nd–Pb isotopic compositions (Figs. 15 and 16). During their ascent to the surface, magmas of the two series underwent variable extents of crustal contamination and fractional crystallization (Hoang et al., 1996; Hoang and Flower, 1998; Koszowska et al., 2007; Barra and Cooper, 2013).

For the Khorat basalts, Zhou and Mukasa (1997) proposed two mantle source domains. One is a moderately depleted mantle similar to the source for Indian MORB and the other is an enriched mantle with an EM2-like isotopic characteristics; these two sources are located in the lithosphere and asthenosphere, respectively. Note, however, that the EM2-like end-member could be coming from a mantle plume, as in the case in Hainan Island (Zou and Fan, 2010 and see below). Variable mixing between enriched mantle plume and depleted lithospheric mantle can produce the Sr, Nd and Pb isotopic characteristics of the Khorat basalts. Trace element characteristics (Fig. 13d and Fig. 14d) further show that the basalts can be produced by low degree partial melting of such mantle sources. During their ascent to the surface, the magmas did not suffer crustal contamination because their trace element geochemical characteristics, i.e., its Nb/Ta = 15.88 (average) and Zr/Hf = 35.78 (average) (Table S2) are close to those of primitive mantle and obviously higher than those continental crust (Sun and McDonough, 1989), but most of them experienced variable degrees of fractional crystallization (Zhou and Mukasa, 1997).

5.4.5. South China Sea

Radiogenic isotope data for the Cenozoic alkalic basalts from Hainan Island suggest that the basalts can be produced by binary mixing (Figs. 15 and 16) between a DMM end-member and an EM2 end-member that may be originating from a plume upwelling from the lower mantle or core/mantle boundary (e.g., Montelli et al., 2006; Zhao, 2007) or from the subcontinental lithospheric mantle (SCLM) (Tu et al., 1992; Fan et al., 2004). It is important to note that a Hainan plume not only provides the heat energy necessary for partial melting of the lithospheric mantle, but also the source material for the magmas (Yan et al., 2008a). Trace element characteristics (Figs. 13e and 14e) show that Hainan basalts may be produced by a low degree of partial melting of their mantle source and have undergone fractional crystallization and/or accumulation during their ascent and storage in shallow level magma chambers. These basalts, including those that were erupted on the northern continental slope around the Zhongsha islands, evidently were not contaminated by continental material, consistent with the fact that they were erupted through an oceanic crust (Yan et al., 2008a; Zou and Fan, 2010).

Flower et al. (1998) once invoked the 'mantle extrusion' model to successfully explain the genesis of dispersed volcanism in east Asia and the western Pacific. However, the model is limited to the scarce of geochemical and geophysical (especially for deep mantle) data. Although there is still in debate for the plume, the presence of Hainan plume recently have been supported by more and more geochemical data mentioned above and geophysical data (Lebedev et al., 2000; Lebedev and Nolet, 2003; Montelli et al., 2006; Zhao, 2007; Lei et al., 2009). So, it is also important to note that the Hainan plume-an upwelling mantle plume may have played an important role in the genesis of some of the Cenozoic basalts, and in the tectonic evolution of the SCS region in general.

6. Tectonic implications

6.1. Does a late Mesozoic Andean-type subduction zone exist in the SCS?

In the Sr/Y–Y variation diagram (Fig. 11), some samples from the Nansha block, Dalat zone and Schwaner Mountain that plot within the TTG (potential modern equivalents – adakites, Martin, 1999) field, the other samples plot in field of the normal arc rocks, indicating that the former may result from partial melting of mixed sources, and the latter may be originated from partial melting of thickened mafic crust with garnet in the residue (Martin, 1995). In the trace element discrimination diagrams of Pearce et al. (1984; Fig. 17a and b), almost all samples from the Nansha micro-block, southern Vietnam and Schwaner Mountains plot within the VAG (volcanic arc granites) field. In the major element diagrams of Maniar and Piccoli (1989; Fig. 18a and b), almost all

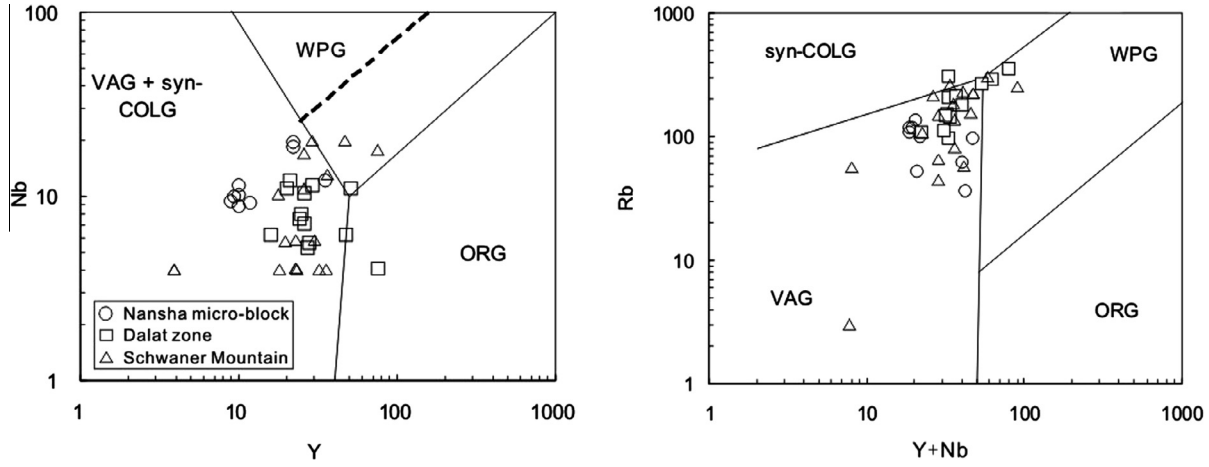

Fig. 17. Trace element discrimination diagrams for late Mesozoic granites in the SCS region (after Pearce et al., 1984). WPG – within plate granite; VAG – Volcanic arc granite; syn-COLG – syn-collisional granite; ORG – oceanic ridge granite.

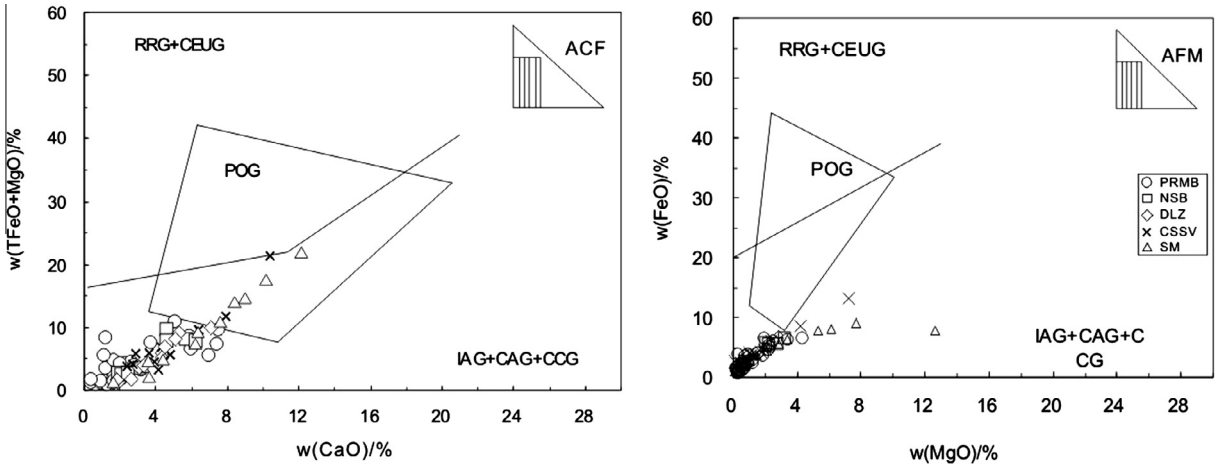

Fig. 18. Major element discrimination diagrams for late Mesozoic granites in the SCS region (after Maniar and Piccoli, 1989). IAG – island arc granite; CAG – continental-arc granite; CCG – continental–collisional granite; POG – post-orogenic granite, RRG – rift-related granite; CEUG – continent-epeirogenic uplift granite. PRMB – Pearl River Mouth Basin; NSB – Nansha micro-block; DLZ – Dalat zone; CSSV – continental shelf in the southern Vietnam; SM – Schwaner Mountains.

samples from the PRMB, Nansha micro-block, continental shelf offshore and onshore southern Vietnam, and Schwaner Mountains plot within the combined IAG (Island arc granites)-CAG (continental arc granites)-CCG (continental collisional granites) field. These characteristic features indicate that these nearly contemporaneous, Late Mesozoic granitic rocks are arc related. This inferred arc tectonic setting, combined with major- and trace element geochemical characteristics for granitic rocks from the SCS region (Figs. 4–9) also indicate that there was no back-arc basin developed behind such an arc, as is typical for Andean-type arcs. Thus, a major conclusion of this study is that it supports the idea that there existed an Andean-type subduction zone in the SCS region during late Mesozoic.

Based on geochemical and geochronological data for granitic rocks compiled in this study, combined with the spatial–temporal distribution of pre-Cenozoic basements in the SCS region (Liu et al., 2011) and various tectonic models presented earlier, the possible present-day traces of the Mesozoic subduction zone within the SCS region can be delineated (Fig. 2), although the evidences is still lacking. Approximately extending southwestward from Taiwan to Borneo, the inferred zone can be divided into six parts. Part no. 1, extending southwestward from offshore southwest Taiwan to the western tip of northwest sub-basin (NWSB), the trace of the subduction zone is similar to that of Holloway (1982). Important arguments for the traces of this part are as follows. Based on geophysical data, Zhou et al. (2008) proposed a buried Mesozoic subduction belt that extends approximately NE45–SW225° from southwest Taiwan Shoal to the northern margin of the SCS deep-sea basin, and this is consistent with the presence of subduction-related Mesozoic granites in the PRMB (Li et al., 1999). Part no. 2, the traces of this part of the subduction zone extends along COB from the western tip of NWSB to the southeast side of Zhongsha micro-block. Important arguments for the traces of this part are the occurrence of subduction-related Mesozoic granites in the Zhongsha micro-block (Jin, 1989; Liu et al., 2002), and Taylor and Hayes (1980, 1983) and Holloway (1982) proposed that the Cenozoic opening of the SCS spilt part of the Mesozoic arc. Part no. 3, the traces in this part is not clear, and the subduction zone connection between the Zhongsha micro-block and north side of Palawan continental terrane (PCT) had been cross-cut by Cenozoic seafloor spreading in the SCS. Part no. 4, extending from the north side of PCT to the eastern tip of the PCT southeastwards then to the land extension site of West Baram line southwestwards.

Important arguments for the traces of this part no. 4 are as follows. 1. PCT once connected with South China block prior to the Cenozoic spreading of the SCS (Rangin et al., 1985). 2. The

basement of NW Palawan trough is continental crust (Hinz and Schlüter, 1985), and ophiolites representing proto-SCS oceanic crust exist in Sabah, northeast Borneo (Hutchison and Vijayan, 2010). 3. The reconstruction of Clift et al. (2008) and Hall (2012) showed micro-blocks (or Luconia–Dangerous Grounds) dispersed in the SCS were rifted from South China, which have been evidenced by the occurrence of subduction-related Mesozoic granites (with similar Pb isotopic compositions to the South China) in the Nansha micro-block which (Yan et al., 2008a,b,c; Yan et al., 2010, 2011).

Part no. 5, the traces in this part is not clear, and this part have been covered by Eocence volcanics, Tertiary and recent sediments (Fuller et al., 1999), and some younger (2.1–4.1 Ma) volcanics (Cullen et al., 2013). Part no. 6, extending from west to east, may lie at the north side of the Schwaner Mountains. Important arguments for the traces of this part are the occurrence of subduction-related Mesozoic granites in the Schwaner Mountains (Williams et al., 1988), the nearly 90° anticlockwise rotation of Borneo since Cretaceous (e.g., Fuller et al., 1999), and Hall's (2012) reconstruction that SW Borneo rifted from Australia also suffered the subduction of Pacific plate during late Mesozoic era which may have produced granitic rocks occurring in the Schwaner Mountains. Although the rotation history of Borneo is still in debate (Haile et al., 1977; Lee and Lawver, 1994; Hall, 1996, 2002; Fuller et al., 1999; Replumaz and Tapponnier, 2003; Cullen et al., 2012), recent paleomagnetic data indicate that Borneo have experienced about 50° anticlockwise rotation during the Cenozoic, and total anticlockwise rotation amplitude may be reached to 90° since Cretaceous (Haile et al., 1977; Fuller et al., 1999; Williams et al., 1988; Hall, 1996, 2002). The rotation history is in accord with many geological features, such as the original NNW orientation of the Schwaner Mesozoic granitic rocks (Hall, 2012) that were possibly connected with the Mesozoic subduction zone mentioned above, but may had been displaced to the present site with E–W orientation by 90° anticlockwise rotation along the Lupar fault.

6.2. Cenozoic geodynamic setting of the SCS

In the Zr/Y vs. Zr tectonic discriminantion diagram (Fig. 19), all SCS Cenozoic volcanics plot within the WPB (intra-plate basalts) field, which indicates that they lie at intra-plate tectonic setting. Moreover, although there is still a debate on the amount of the extrusion, it is widely agreed that SE Asia was extruded from the south China block when India collided with Eurasia during the late

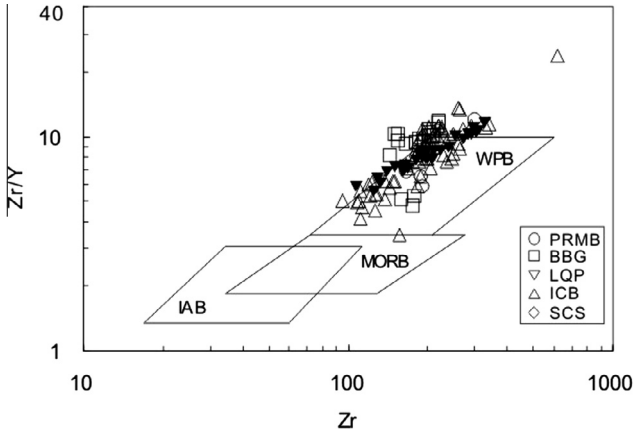

Fig. 19. Zr/Y vs. Zr tectonic discriminantion diagrams for the Cenozoic volcanics from the SCS region. WPB – within plate basalt; MORB – mid-ocean ridge basalt; IAB – island arc basalt. PRMB – Pearl River mouth basin; BBG – Beibu gulf; LQP – Leiqiong peninsula; ICB – Indochina block; SCS – South China Sea.

Cenozoic (e.g., Tapponnier, 1986; Replumaz and Tapponnier, 2003; Hall et al., 2008; Clift et al., 2008). This collision process between the Indian and Eurasian plate influenced the SCS region. That is, the integrated effects of the collision between India and Eurasian plate since the Eocene and the ocean-ward gradual retreat of the Paleo-pacific subduction zone since mid-Cretaceous created an extensional tectonic setting in the SCS region. In the northern margin of the SCS, there are a series of Tertiary rifted basins (Li et al., 1998; e.g., Qiongdongnan basin, PRMB, southwest Taiwan basin, and Sanshui basin, Lianping basin and Heyuan basin in Guangdong provinces) where bimodal volcanism (60–43 Ma until 24 Ma for the PRMB) was widespread (Zou et al., 1995; Chung et al., 1997; Zhou et al., 2009) in response to the overall extensional geodynamic setting. Based on the petrological and geochemical data of Cenozoic volcanic rocks, however, Zhou et al. (2009) suggested that an upwelling mantle plume may be the dominant driving force for the bimodal volcanism in Sanshui basin.

During Cenozoic seafloor spreading in the SCS (37 or 32–16 Ma; Hsu et al., 2004; Cande and Kent, 1995), melts formed by the adiabatically decompressing mantle beneath the spreading centers created the seafloor. Hence the period from ca. 37 or 32 Ma to ca. 16 Ma, which is commonly referred to as magmatically quiet period, is in fact a time of voluminous volcanism which created the basin crust that is now covered by thick sediments.

After the cessation of Cenozoic seafloor spreading, the oceanic crust began to subduct beneath the Philippine arc, forming a volcanic arc in Taiwan and Luzon (Defant et al., 1989, 1990). Meanwhile, widespread intraplate volcanism (17 Ma to present) occurred in the Leiqiong peninsula, BBG, Indochina block, and within the SCS. Geochemical data indicate that the intraplate volcanics received a major contribution from the Hainan mantle plume, and this is consistent with geophysical data (e.g., Lebedev and Nolet, 2003; Montelli et al., 2006; Zhao, 2007; Lei et al., 2009).

The existence of the Hainan plume is supported by geochemical and geophysical data. Seismic tomographic data indicate that a sub-vertical low-velocity column is imaged beneath the Hainan Island and the South China Sea and extends from shallow depths down to the 660-km discontinuity (Lebedev et al., 2000; Lebedev and Nolet, 2003), and the latest data show that the Hainan plume may extend to mid-mantle depths and may be a dying plume (Montelli et al., 2006). ^{230}Th excesses in Hainan lavas also suggest a slowly (<1 cm/year) rising mantle plume (Zou and Fan, 2010). Based on whole-mantle tomographic images, Zhao (2007) pointed out that the Hainan mantle plume is one of the twelve mantle plumes which originated from the core–mantle boundary. Lei et al. (2009) further suggested that the Hainan plume is a continuous, NW–SE tilting, low-V column with a diameter of about 80 km, from the surface down to 250 km depth. Similar low-velocity column below the South China Sea region had also been discovered by Cai et al. (2010) on the basis of new geophysical data. In addition, the compiled petrological and geochemical data in this study (Table 2; Figs. 12–16), e.g., bimodal volcanism in Sanshui, Lianping and Heyuan basins (Zhou et al., 2009) and earlier bimodal volcanism and later alkalic (dominantly) basaltic magmas (Zou et al., 1995), and basaltic rocks from Beibu gulf (Jia et al., 2003; Li et al., 2005), Indochina block (Zhou and Mukasa, 1997; Hoang and Flower, 1998), Leiqiong peninsula (Zhu and Wang, 1989; Zou and Fan, 2010; Wang et al., 2012, 2013), and seamounts in the SCS (Yan et al., 2008a; Xu et al., 2012), reflect that all of them need an enriched end-member in the mantle source, implying the existence of a mantle plume in the SCS region. The above evidences, combined with results achieved by integrated study on the tectonic, basin filling and thermal evolution of those Tertiary rifted basins in the northern margin of the SCS (Li et al., 1998), suggests that the Hainan plume may play a significant role for tectonic evolution of the SCS region. However, although there are some

geochemical and geophysical evidences for the existence of the Hainan mantle plume, there is still a need to further constrain the evolutionary history of the plume.

6.3. A tectono-magmatic evolution model for the SCS region since late Mesozoic

Pb isotopic composition of Mesozoic granitic rocks from the Nansha block which is considered a good representative of the micro-blocks in the SCS basin, indicates that it has tectonic affinity with the south China block (Yan et al., 2011). Other few emerging petrologic and geochemical data also indicate a similar affinity for the other blocks. Thus, the micro-blocks were most probably once contiguous with the south China block during the Permian or Triassic, and the latter block, together with those various pre-Cretaceous continental terranes of east and southeast Asia, have been considered as all derived directly or indirectly from Gondwanaland (Metcalfe, 1996, 2011a, 2011b; Yu et al., 2008; Cullen, 2014). An Andean-type subduction zone existed at the southeast side of these micro-blocks, Taiwan, offshore southern Vietnam and Schwaner Mountains during the late Mesozoic era. The proto-SCS formed at the northwest side of the subduction zone (Hutchison et al., 2000; Cullen, 2014).

Since the earlier Paleogene (~56 Ma), when the leading edge of the India plate reached the Eurasian plate (e.g., Zhu et al., 2004), these micro-blocks began to rift from the south China block and rifted away from each other along ancient faults (or sutures). Meanwhile, the proto-SCS began to subduct beneath the Borneo (Cullen, 2014), forming an Andean-type arc, which implies a reveral and jump in the location of the Proto-SCS subduction zone. The overall tectonic setting of the northern passive margin of the SCS has always been extensional and a series of Tertiary rifted basins formed there. Some investigators suggested that the Cenozoic seafloor spreading in the SCS initiated at the pre-existing Andean-type arc.

Although the mantle plume did not appear to exert a major control on rifting, it played a significant role in the formation of rifted basins (e.g., Coffin and Eldholm, 1994; Ziegler and Cloetingh, 2004), as indicated by the compositional signature of the accompanying bimodal volcanism (e.g., Roy, 2001) and in the upwelling of asthenospheric mantle (e.g., Ziegler and Cloetingh, 2004). Indeed, Storey (1995) proposed that mantle plumes have played an important role in the continental break-up of Gondwanaland. Here we also assume that the Hainan mantle plume initiated in earlier Cenozoic and played an important role in the plate tectonic evolution of the SCS region.

The details of our evolutionary model are as follows. (1) 50–30 Ma: The collision between Indian and Euro-Asian plates and eastward retrogression of the Pacific plate created an extensional tectonic setting in east Asia including the SCS region; it also triggered the upwelling of the Hainan mantle plume. Bimodal volcanism in the northern margin of the SCS provides evidence for the activity of the plume. (2) 37 or 30–16 Ma: When the head of the Hainan mantle plume arrived in the asthenosphere, it immediately interacted with the spreading center of the South China Sea through lateral flow beneath the rigid lithosphere, enhancing spreading rate, causing at least two episodes of ridge jumps (one at 26–24 Ma – Briais et al., 1993 and the other at 21 Ma – Pautot et al., 1986) as well as asymmetric spreading as evidenced in the magnetic anomaly patterns (Briais et al., 1993). (3) 16–0 Ma: After proto-SCS crust was completely subducted, continental crust began to enter the subduction zone on the NW margin of Borneo, and seafloor spreading in the SCS stopped. Subsequently, the earlier formed oceanic crust subducted along the Manila trench. The Hainan mantle plume is currently active, producing large amounts of alkalic basalts in the SCS region. It must be noted that the discovery of high-velocity layer (with velocities of 8.2–8.4 km/s) at depth of 60–80 km under the SCS basin (Yao and Wan, 2010) may possibly be due to a later-period (especially during post-spreading period) of underplating of asthenospheric melts that flowed laterally from the Hainan mantle plume.

7. Summary and conclusions

Available petrologic, geochonologic and geochemical data for late Mesozoic to Recent igneous rocks in the SCS region have been reviewed and combined with all other geologic information in order to construct an integrated tectono-magmatic evolutionary model for the entire region. Results of our investigation show that available data support the proposal by Holloway (1982) and Taylor and Hayes (1980, 1983) that a late Mesozoic Andean-type volcanic arc existed in this region due to the subduction of proto-Pacific plate. The occurrence of mainly I-type granitic rocks along the presumed continental arc is consistent with this model. In the northern margin of the SCS, the early Cenozoic was characterized by bimodal type of volcanism and Hainan mantle plume magmatism; the latter may have played a significant role in the tectonic evolution of the rifted basins in this region. Seafloor spreading followed at 37 or 30–16 Ma and the Hainan mantle plume interacted with the spreading center. After the cessation of seafloor spreading in the SCS, arc magmatism commenced along the eastern margin of the basin and widespread magmatism associated with mantle plume occurred throughout the SCS region. As mentioned earlier, there did not obtain samples representing oceanic crust basement of the SCS so far, and we did not know much about the nature of mantle beneath the SCS and its accurate spreading period from direct dating on oceanic crust samples. So, some fundamental problems that should be addressed in future research efforts, e.g., sampling the SCS crust (Li et al., 2013), more isotopic studies on mantle xenoliths and igneous rocks, etc.

Acknowledgements

We are very grateful to Chris Morley and Andrew Cullen for their reviewing the manuscript and Bor-ming Jahn for editorial handling; their detailed comments and suggestions greatly improve the manuscript. This work was supported by the National Natural Science Foundation of China under contract Nos. 41322036, 41230960, and 41276003, China Ocean Mineral Resources R&D Association (COMRA) under Contract No. DY125-12-R-05, China Postdoctoral Science Foundation under Contract No. 201104616, and the Taishan Scholar Program of Shandong Province.

Appendix A. Supplementary material

Supplementary data associated with this article can be found, in the online version, at http://dx.doi.org/10.1016/j.jseaes.2014.02.005.

References

Areshev, E.G., Dong, T.L., San, N.T., Shnip, O.A., 1992. Reservoirs in fractured basement on the continental shelf of southern Vietnam. J. Pet. Geol 15 (4), 451–464.

Arfai, J., Franke, D., Gaedicke, C., Lutz, R., Schnabel, M., Ladage, S., Berglar, K., Aurelio, M., Montano, J., Pellejera, N., 2011. Geological evolution of the West Luzon Basin (South China Sea, Philippines). Mar. Geophys. Res. 32, 349–362.

Baksi, A.K., 2003. Critical evaluation of $^{40}Ar/^{39}Ar$ ages for the central atlantic magmatic province. Timing, duration and possible migration of magmatic centers. Am. Geophys. Union Monogr. 136, 77–90.

Barckhausen, U., Roeser, H.A., 2004. Seafloor spreading anomalies in the South China Sea revisited. In: Clift, P., Wang, P., Kuhnt, W., Hayes, D. (Eds.), Continent–Ocean Interactions with East Asian Marginal Seas, vol. 140. American Geophysical Union, pp. 121–125.

Barra, S.M., Cooper, M.A., 2013. Late Cenozoic basalt and gabbro in the subsurface in the Phetchabun Basin, Thailand: implications for the Southeast Asian Volcanic Province. J. Asian Earth Sci. 76, 169–184.
Braitenberg, C., Wienecke, S., Wang, Y., 2006. Basement, structures from satellite-derived gravity field: South China Sea Ridge. J. Geophys. Res. 111, B05407. http://dx.doi.org/10.1029/2005JB003938.
Briais, A., Patriat, P., Tapponier, P., 1993. Updated interpretation of magnetic anomalies and seafloor spreading stages in the South China Sea: implications for the Tertiary tectonics of Southeast Asia. J. Geophys. Res. 98 (B4), 6299–6328.
Cai, X., Zhu, J., Cheng, X., Cao, J., 2010. The structure of the composite mushroom-shaped mantle plume in the South China Sea and its mantle dynamics. Geol. China 37 (2), 268–279 (in Chinese with English abstract).
Cande, S.C., Kent, D.V., 1995. Revised calibration of the geomagnetic polarity timescale for the Late Cretaceous and Cenozoic. J. Geophys. Res. 98, 6299–6328.
Castillo, P., 1988. The Dupal anomaly as a trace of the upwelling lower mantle. Nature 336, 667–670.
Castillo, P., 1996. Origin and geodynamic implication of the Dupal isotopic anomaly in volcanic rocks from the Philippine island arcs. Geology 24, 271–274.
Chung, S.L., 1999. Trace element and isotope characteristics of Cenozoic basalts around the Tanlu Fault with implication for the eastern plate boundary between north and south China. J. Geol. 107, 301–312.
Chung, S.L., Cheng, H., Jahn, B.M., O'Reilly, S.Y., Zhu, B.Q., 1997. Major and trace element, and Sr–Nd isotope constraints on the origin of Paleogene volcanism in South China prior to the South China Sea opening. Lithos 40, 203–220.
Clift, P., Lee, G.H., Anh Duc, N., Barckhausen, U., Van Long, H., Zhen, S., 2008. Seismic reflection evidence for a Dangerous Grounds miniplate: no extrusion origin for the South China Sea. Tectonics 27, TC3008. http://dx.doi.org/10.1029/2007TC002216.
Coffin, M.E., Eldholm, O., 1994. Large igneous provinces: crustal structure, dimensions, and external consequences. Rev. Geophys. 32, 1–36.
Cullen, A., 2010. Transverse segmentation of the Baram–Balabac Basin, NW Borneo: refining the model of Borneo's tectonic evolution. Petrol. Geosci. 16, 3–29.
Cullen, A., 2014. Nature and significance of the West Baram and Tinjar lines: NW Borneo. Mar. Pet. Geol. 51, 197–209.
Cullen, A., Zechmeister, M., Elmore, R., Pannalal, S., 2012. Paleomagnetism of the Crocker Formation, northwest Borneo: Implications for late Cenozoic tectonics. Geosphere 8, 1146–1169.
Cullen, A., Macpherson, C., Taib, N.I., Burton-Johnson, A., Geist, D., Spell, T., Banda, R.M., 2013. Age and petrology of the Usun Apau and Linau Balui volcanics: windows to central Borneo's interior. J. Asian Earth Sci. 76, 372–388.
Cuong, T., Warren, J., 2009. Bach Ho Field, a fractured granitic basement reservoir, Cuu Long Basin, Offshore SE Vietnam: a "Buried Hill" play. J. Pet. Geol 32, 129–156.
Defant, M.J., Jacques, D., Maury, R.C., De Boer, J., Joron, J.L., 1989. Geochemistry and tectonic setting of the Luzon arc, Philippines. Geol. Soc. Am. Bull. 101, 663–672.
Defant, M.J., Maury, R., Joron, J.L., Feigenson, M.D., Leterrier, J., Bellon, H., Jacques, D., Richard, M., 1990. The geochemistry and tectonic setting of the northern section of the Luzon arc (the Philippines and Taiwan). Tectonophysics 183, 187–205.
Fan, Q.C., Sun, Q., Li, N., Sui, J.L., 2004. Periods of volcanic activity and magma evolution during Holocene in the northern Hainan Island. Acta Petrol. Sin. 20, 533–544 (in Chinese with English abstract).
Faure, G., 1986. Principle of Isotope Geology, second ed. John Wiley and Sons, New York., p. 589.
Flower, M.F.J., Zhang, M., Chen, C.Y., Tu, K., Xie, G.H., 1992. Magmatism in the South China Basin 2. Post-spreading Quaternary basalts from Hainan Island, south China. Chem. Geol. 97, 65–87.
Flower, M.F.J., Tamaki, K., Hoang, N., 1998. Mantle extrusion: a model for dispersed volcanism and DUPAL-like asthenosphere in east Asia and the western Pacific. In: Flower, M.F.J., Chung, S.-L., Lo, C.-H., Lee, T.-Y. (Eds.), Mantle Dynamics and Plate Interactions in East Asia. American Geophysical Union, Washington, pp. 67–88.
Fuller, M., Ali, J.R., Moss, S.J., Frost, G.M., Richter, B., Mahfi, A., 1999. Paleomagnetism of Borneo. J. Asian Earth Sci. 17, 3–24.
Haile, N.S., McElhinny, M.W., McDougall, I., 1977. Palaeomagnetic data and radiometric ages from the cretaceous of west Kalimantan (Borneo), and their significance in interpreting regional structure. J. Geol. Soc. Lond. 133, 133–144.
Hall, R., 1996. Reconstructing Cenozoic SE Asia. In: Hall, R., Blundell, D. (Eds.), Tectonic Evolution of Southeast Asia, vol. 106. Geological Society of London Special Publication, pp. 153–184.
Hall, R., 2002. Cenozoic geological and plate tectonic evolution of SE Asia and the SW Pacific: computer-based reconstructions, model and animations. J. Asian Earth Sci. 20, 353–431.
Hall, R., 2012. Late Jurassic–Cenozoic reconstructions of the Indonesian region and the Indian Ocean. Tectonophysics 570, 1–41.
Hall, R., van Hattum, M.W.A., Spakman, W., 2008. Impact of India–Asia collision on SE Asia: the record in Borneo. Tectonophysics 451, 366–389.
Hall, R., Clements, B., Smyth, H.R., 2009. Sundaland: basement character, structure and plate tectonic development. In: Proceedings, Indonesian Petroleum Association Thirty-Third Annual Convention and Exhibition, May 2009.
Hamelin, B., Allègre, C.J., 1985. Large scale regional units in the depleted upper mantle revealed by an isotopic study of the south-west Indian ridge. Nature 315, 196–199.
Hamilton, W., 1979. Tectonics of the Indonesian region. U.S. Geol. Surv. Prof. Pap. 1078, 345.
Hart, S.R., 1984. A large-scale isotope anomaly in the Southern Hemisphere mantle. Nature 309, 753–757.
Hawkesworth, C.J., Kemp, A.I.S., 2006. Evolution of the continental crust. Nature 443, 811–817.
He, L., 1988. Formation and petroleum of South China Sea. Mar. Geol. Quat. Geol. 8 (2), 15–28 (in Chinese with English abstract).
Hickey-Vargas, R., Hergt, J.M., Spadea, P., 1995. The Indian Ocean-type isotopic signature in western Pacific marginal basins: origin and significance. Active Marg. Marg. Basins Western Pacif. Geophys. Monogr. 88, 175–197.
Hinz, K., Schlüter, H.U., 1985. Geology of the dangerous grounds, South China Sea, and the continental margin off Southwest Palawan: results of SONNE cruises SO-23 and SO-27. Energy 10, 297–315.
Hoang, N., Flower, M., 1998. Petrogenesis of Cenozoic Basalts from Vietnam: Implication for Origins of a 'Diffuse Igneous Province'. J. Petrol. 39 (3), 369–395.
Hoang, N., Flower, M., Carlson, R.W., 1996. Major, trace element, and isotopic compositions of Vietnamese basalts: interaction of hydrous EM1-rich asthenosphere with thinned Eurasian lithosphere. Geochim. Cosmochim. Acta 60 (22), 4329–4351.
Hofmann, A.W., 1988. Chemical differentiation of the Earth: the relationship between mantle, continental crust and oceanic crust. Earth Planet. Sci. Lett. 90, 297–314.
Hofmann, A.W., 1997. Mantle geochemistry – the message from oceanic volcanism. Nature 385, 219–229.
Holloway, N.H., 1982. North Palawan block, Philippine-its relation to Asian mainland and role in evolution of South China Sea. Bull. Am. Assoc. Petrol. Geolog. 66, 1355–1383.
Honza, E., 1995. Spreading mode of backarc basins in the western Pacific. Tectonophysics 251, 139–152.
Honza, E., Fujioka, K., 2004. Formation of arcs and backarc basins inferred from the tectonic evolution of Southeast Asia since the Late Cretaceous. Tectonophysics 384, 23–53.
Hsu, S.-K., Yeh, Y.-C., Doo, W.-B., Tsai, C.-H., 2004. New bathymetry and magnetic lineations identifications in the northernmost South China Sea and their tectonic implications. Mar. Geophys. Res. 25, 29–44.
Hutchison, C.S., 2004. Marginal basin evolution: the southern South China Sea. Mar. Pet. Geol. 21, 1129–1148.
Hutchison, C.S., 2005. Geology of NW Borneo: Sarawak. Elsevier, Brunei and Sabah, p. 444.
Hutchison, C.S., Vijayan, V.R., 2010. What are the Spratly Islands? J. Asian Earth Sci. 39, 371–385.
Hutchison, C.S., Bergman, S.C., Swauger, D.A., Graves, G.E., 2000. A Miocene collisional belt in north Borneo: uplift mechanism and isostatic adjustment quantified by thermochronology. J. Geol. Soc. 157, 783–793.
Irvine, T.N., Baragar, W.R.A., 1971. A guide to the chemical classification of the common volcanic rocks. Can. J. Earth Sci. 8, 523–548.
Jahn, B.M., 1974. Mesozoic thermal events in Southeast China. Nature 248, 480–483.
Jahn, B.M., Zhou, X.H., Li, J.L., 1990. Formation and tectonic evolution of southeastern China and Taiwan: isotopic and geochemical constraints. Tectonophysics 183, 145–160.
Jia, D.C., Qiu, X.L., Hu, R.Z., Lu, Y., 2003. Geochemical nature of mantle reservoirs and tectonic setting of basalts in Beibu gulf and its adjacent region. J. Trop. Oceanogr. 22 (2), 30–39 (in Chinese with English abstract).
Jin, X.L., 1989. The geosciences research report in South China Sea. Donghai Mar. Sci. 7 (4), 30–42 (in Chinese).
Karig, D.E., 1971. Origin and development of marginal basin in the western Pacific. J. Geophys. Res. 76, 2543–2561.
Knittel, U., 2011. 83 Ma rhyolite from Mindoro – evidence for Late Yanshanian magmatism in the Palawan Continental Terrane (Philippines). Island Arc 20, 138–146.
Knittel, U., Trudu, A.G., Winter, W., Yang, T.F., Gray, C.M., 1995. Volcanism above a subducted extinct spreading center: a reconnaissance study of the North Luzon Segment of the Taiwan-Luzon Volcanic Arc (Philippines). J. SE Asian Earth Sci. 11 (2), 95–109.
Koszowska, E., Wolska, A., Zuchiewicz, W., Cuong, N., Pécskay, Z., 2007. Crustal contamination of Late Neogene basalts in the Dien Bien Phu Basin, NW Vietnam: some insights from petrological and geochronological studies. J. Asian Earth Sci. 29, 1–17.
Kudrass, H.R., Wiedicke, M., Cepek, P., Kreuzer, H., Müller, P., 1986. Mesozoic and Cainozoic rocks dredged from the South China Sea (Reed Bank area) and Sulu Sea and their significance for plate-tectonic reconstructions. Mar. Pet. Geol. 3 (1), 19–30.
Lan, C.Y., Jahn, B.M., Mertzmant, S.A., Wu, T.W., 1996. Subduction-related granitic rocks of Taiwan. J. SE Asian Earth Sci. 14, 11–28.
Lan, C.Y., Chung, S.L., Van Long, T., Lo, C.H., Lee, T.Y., Mertzmane, S.A., Shen, J.J.S., 2003. Geochemical and Sr–Nd isotopic constraints from the Kontum massif, central Vietnam on the crustal evolution of the Indochina block. Precambr. Res. 122, 7–27.
Le Maitre, R.W. (Ed.), 1989. A Classification of Igneous Rocks and Glossary of Terms. Blackwell, Oxford, pp. 193.
Lebedev, S., Nolet, G., 2003. Upper mantle beneath Southeast Asia from S velocity tomography. J. Geophys. Res. 108 (B1), 20–48.
Lebedev, S., Chevrot S, Nolet G., van Hilst R.D., 2000. New seismic evidence for a deep mantle origin of the S. China basalts (the Hainan Plume?) and other observations in SE Asia. EOS Trans. Am. Geophys. Union 81(48) (Fall Meeting Supplement).
Lee, T.Y., Lawver, L.A., 1994. Cenozoic plate reconstruction of the South China Sea region. Tectonophysics 235, 149–180.

Lee, T.Y., Lo, C.H., Chung, S.L., Chen, C.Y., Wang, P.L., Nguyen, H., Cumg, T.C., Nguyen, T.Y., 1998. $^{40}Ar/^{39}Ar$ dating result of Neogene basalts in Vietnam and its tectonic implication. Am. Geophys. Union, Geodyn. Ser. (Mantle Dyn. Plate Interact. East Asia) 27, 317–330.

Lei, J., Zhao, D., Steinberger, B., Wu, B., Shen, F., Li, Z., 2009. New seismic constraints on the upper mantle structure of the Hainan plume. Phys. Earth Planet. Inter. 173, 33–50.

Li, X.H., 2000. Cretaceous magmatism and lithospheric extension in Southeast China. J. Asian Earth Sci. 18, 293–305.

Li, Z.X., Li, X.H., 2007. Formation of the 1300-km-wide intracontinental orogen and postorogenic magmatic province in Mesozoic South China: a flat-slab subduction model. Geology 35 (2), 179–182.

Li, P.L., Rao, C.T., 1994. Tectonic characteristics and evolution history of the Pearl River Mouth Basin. Tectonophysics 235, 13–25.

Li, S.T., Lin, C.S., Zhang, Q.M., Yang, S.G., Wu, P.K., 1998. Dynamic process of episodic rifting in continental marginal basin and tectonic events since 10 Ma in South China Sea. Chin. Sci. Bull. 43 (8), 797–810 (in Chinese).

Li, P.L., Liang, H.X., Dai, Y.D., Lin, H.M., 1999. Origin and tectonic setting of the Yanshanian igneous rocks in the Pearl River Mouth basin. Guangdong Geol. 14 (1), 1–8 (in Chinese with English Abstract).

Li, C.N., Wang, F.Z., Zhong, C.S., 2005. Geochemistry of Quaternary basaltic volcanic rocks of Weizhou island in Beihai city of Guangxi and a discussion on characteristics of their source. Acta Petrol. Mineral. 24 (1), 1–11 (in Chinese with English abstract).

Li, X.H., Li, W.X., Li, Z.X., 2007. On the genetic classification and tectonic implications of the Early Yanshanian granitoids in the Nanling Range, South China. Chin. Sci. Bull. 52, 1873–1885.

Li, C.-F., Lin, J., Kulhanek, D.K., 2013. South China Sea tectonics: opening of the South China Sea and its implications for southeast Asian tectonics, climates, and deep mantle processes since the late Mesozoic. IODP Sci. Prosp. 349. http://dx.doi.org/10.2204/iodp.sp.349.2013.

Liu, Z.S., Zhao, H.T., Fan, S.Q., Chen, S.Q., 2002. Geology of the South China Sea. Science Press, Beijing, China, pp. 1–5.

Liu, H.L., Yan, P., Liu, Y.C., Deng, H., 2006. Discussion on the existence of Qiongnan suture in the northern margin of the South China Sea and its implications. Chin. Sci. Bull. 51 (Suppl.), 92–101 (in Chinese with English abstract).

Liu, H., Zheng, H., Wang, Y., Lin, Q., Wu, C., Zhao, M., Du, Y., 2011. Basement of the South China Sea area: tracing the Tethyan realm. Acta Geol. Sinica 85 (3), 637–655.

Lu, W., 1987. Magnetic anomalies and structural evolution of the central subbasin of South China Sea. Acta Oceanol. Sin. 9 (1), 69–78 (in Chinese with English abstract).

Mahoney, J.J., Natland, J.H., White, W.M., Poreda, R., Bloomer, S.H., Flsher, R.L., Baxter, A.N., 1989. Isotopic and geochemical provinces of western Indian Ocean spreading centers. J. Geophys. Res. 94, 4033–4052.

Maniar, P.D., Piccoli, P.M., 1989. Tectonic discrimination of granitoids. Geol. Soc. Am. Bull. 101, 635–643.

Martin, H., 1995. The Archaean grey gneisses and the genesis of the continental crust. In: Condie, K.C. (Ed.), The Archaean Crustal Evolution. Elsevier, pp. 205–259.

Martin, M., 1999. Adakitic magmas: modern analogues of Archaean granitoids. Lithos 46, 411–429.

McCulloch, M.T., Chappell, B.W., 1982. Nd isotopic characteristics of S- and I-type granites. Earth Planet. Sci. Lett. 58, 51–64.

Metcalfe, I., 1996. Pre-Cretaceous evolution of SE Asian terranes. In: Hall, R., Blundell, D. (Eds.), Tectonic Evolution of Southeast Asia, vol. 106. Geology Society of London Special Publication, pp. 97–122.

Metcalfe, I., 2011a. Tectonic framework and Phanerozoic evolution of Sundaland. Gondwana Res. 19, 3–21.

Metcalfe, I., 2011b. Palaeozoic–Mesozoic history of SE Asia. Geol. Soc. Lond. Spec. Publ. 355, 7–35.

Montelli, R., Nolet, G., Dahlen, F.A., Masters, G., 2006. A catalogue of deep mantle plumes: new results from finite frequency tomography. Geochem. Geophys. Geosyst. 7, Q11007. http://dx.doi.org/10.1029/2006GC001248.

Morley, C.K., 2012. Late cretaceous–early Palaeogene tectonic development of SE Asia. Earth Sci. Rev. 115, 37–75.

Morley, C.K., 2013. Discussion of tectonic models for Cenozoic strike-slip fault-affected continental margins of mainland SE Asia. J. Asian Earth Sci. 76, 137–151.

Muir, R.G., Weaver, S.D., Bradshaw, J.D., Eby, G.N., Ewans, J.A., 1995. Geochemistry of the Cretaceous separation point batholiths, New Zealand: granitoid magmas formed by melting of mafic lithosphere. J. Geol. Soc. Lond. 152, 689–701.

Nam, T.N., Yuji, S., Kentaro, T., Mitsuhiro, T., Quynh, P.V., Dung, L.T., 2001. First SHRIMP U–Pb dating of granulites from the Kontum massif (Vietnam) and tectonothermal implications. J. Asian Earth Sci. 19, 77–84.

Nguyen, T.B.T., Satir, M., Siebel, W., Vennemann, T., Trinh, V.L., 2004a. Geochemical and isotopic constraints on the petrogenesis of granitoids from the Dalat zone, southern Vietnam. J. Asian Earth Sci. 23, 467–482.

Nguyen, T.B.T., Satir, M., Siebel, W., Chen, F., 2004b. Granitoids in the Dalat zone, southern Vietnam: age constraints on magmatism and regional geological implications. Int. J. Earth Sci. (Geol. Rundsch) 93, 329–340.

Niu, Y.L., O'Hara, M.J., 2003. Origin of ocean island basalts: a new perspective from petrology, geochemistry, and mineral physics considerations. J. Geophys. Res. 108 (B4), 5–19.

Pautot, G., Rantin, C., Briais, A., Tapponnier, P., Beuzart, P., Lericolais, G., Mathieu, X., Wu, J., Han, S., Li, H., Lu, Y., Zhao, J., 1986. Spreading direction in the South China Sea. Nature 321, 151–154.

Pearce, J.A., Narris, N.B.W., Tindle, A.G., 1984. Trace element discrimination diagrams for the tectonic interpretation of granitic rocks. J. Petrol. 25, 956–983.

Rangin, C., Stephan, J.F., Müller, C., 1985. Middle Oligocene oceanic crust of South China Sea jammed into Mindoro collision zone (Philippines). Geology 13, 425–428.

Replumaz, A., Tapponnier, P., 2003. Reconstruction of the deformed collision zone between India and Asia by backward motion of lithospheric blocks. J. Geophys. Res. 108 (B6), 2285. http://dx.doi.org/10.1029/2001JB000661.

Roy, A.B., 2001. Neoproteozoic crustal evolution of northwestern Indian shield: implication on break up and assembly of Supercontinents. Gondwana Res. 4, 289–306.

Ru, K., Piggot, J.D., 1986. Episodic rifting and subsidence in the South China Sea. Bull. Am. Assoc. Petrol. Geolog. 70 (9), 1136–1155.

Rudnick, R.L., Gao, S., 2003. The composition of the continental crust. In: Rudnick, R.L. (Ed.), The Crust, vol. 3. In: Holland, H.D., Turekian, K.K. (Eds.), Treatise on Geochemistry. Elsevier-Pergamon, Oxford, pp. 1–64. .

Schluter, H.U., Hinz, K., Block, M., 1996. Tectono-stratigraphic terranes and detachment faulting of the South China Sea and Sulu Sea. Mar. Geol. 130, 39–78.

Shipboard Scientific Party, 2000. Site 1143. In: Wang, P., Prell, W.L., Blum, P., et al. (Eds.), Proc. ODP, Init. Repts. 184, pp. 1–103 ([CD-R] available from: Ocean Drilling Program, Texas A&M University, College Station, Texas 77845-9547, USA).

Staudigel, P., Zindler, A., Hart, S.R., Leslie, T., Chen, C.Y., Clague, D., 1984. The isotope systematics of a juvenile intra-plate volcano: Pb, Nd and Sr isotope ratios of basalts from loihi Seamount. Hawaii. Earth Planet. Sci. Lett. 69, 13–29.

Storey, B.C., 1995. The role of mantle plumes in continental break-up: case histories from Gondwanaland. Nature 377, 301–308.

Sun, S.S., McDonough, W.F., 1989. Chemical and isotopic systemtics of oceanic basalts: Implications of mantle composition and processes. Geol. Soc. Lond. Spec. Publ. 42, 313–345.

Tapponnier, P., 1986. On the mechanics of the collision between India and Asia. Geol. Soc. Spec. Publ. 19, 115–157.

Taylor, B., Hayes, D.E., 1980. The tectonic evolution of the South China Sea Basin. In: Hayes, D.E. (Ed.), The Tectonic and Geologic Evolution of Southeast Asia Seas and Islands. Geophysical Monograph Series 23. AGU, Washington, DC.

Taylor, B., Hayes, D.E., 1983. Origin and history of the South China Sea Basin. In: Hayes, D.E. (Ed.), The Tectonic and Geologic Evolution of Southeast Asia Seas and Islands. 2. Geophysical Monograph Series 27. AGU, Washington, DC.

Taylor, S.R., McLennan, S.M., 1985. The Continental Crust: Its Composition and Evolution. Blackwell, Oxford, p. 328.

Tiepolo, M., Bottazzi, P., Foley, S.F., Oberti, R., Vannucci, R., Zanetti, A., 2001. Fractionation of Nb and Ta from Zr and Hf at mantle depths: the role of titanian pargasite and kaersutite. J. Petrol. 42, 221–232.

Tingay, M., Morley, C., King, R., Hillis, R., Coblentz, D., Hall, R., 2010. Present-day stress field of Southeast Asia. Tectonophysics 482, 92–104.

Tu, K., Flower, M.F.J., Carlson, R.W., Zhang, M., Xie, G., 1991. Sr, Nd, and Pb isotopic compositions of Hainan basalts (south China): implications for a subcontinental lithosphere Dupal source. Geology 19, 567–569.

Tu, K., Flower, M.F.J., Carlson, R.W., Xie, G.H., Chen, C.Y., Zhang, M., 1992. Magmatism in the South China Basin, 1. Isotopic and trace element evidence for an endogenous Dupal mantle component. Chem. Geol. 97, 47–63.

Wang, X.J., Wu, M.Q., Liang, D.H., Yin, A.W., 1984. Some geochemical characteristics of basalts from the South China Sea. Geochemica 4, 332–340 (in Chinese with English abstract).

Wang, X., Li, Z., Li, X., Li, J., Long, W., Liu, Y., Zhou, J.B., Wang, F., 2012. Temperature, pressure, and composition of the mantle source region of late Cenozoic basalts in Hainan Island, SE Asia: a consequence of a young thermal mantle plume close to subduction zones? J. Petrol. 53, 177–233.

Wang, X., Li, Z., Li, X., Li, J., Xu, Y.G., Li, X.H., 2013. Identification of an ancient mantle reservoir and young recycled materials in the source region of a young mantle plume: implications for potential linkages between plume and plate tectonics. Earth Planet. Sci. Lett. 377–378, 248–259.

White, A.J.R., Chappell, B.W., 1983. Granitoid types and their distribution in the Lachlan Fold Belt, southeastern Australia. Geol. Soc. Am. Mem. 159, 21–34.

Williams, P.R., Johnston, C.R., Almond, R.A., Simamora, W.H., 1988. Late Cretaceous to Early Tertiary structural elements of West Kalimantan. Tectonophysics 148, 279–297.

Wu, F.Y., Lin, J.Q., Wilde, S.A., Zhang, X.O., Yang, J.H., 2005. Nature and significance of the Early Cretaceous giant igneous event in eastern China. Earth Planet. Sci. Lett. 233, 103–119.

Xu, Y.G., Wei, J.X., Qiu, H.N., Zhang, H.H., Huang, X.L., 2012. Opening and evolution of the South China Sea constrained by studies on volcanic rocks: preliminary results and a research design. Chin. Sci. Bull. 57, 3150–3164.

Yan, Q.S., Shi, X.F., 2007. Hainan mantle plume and the formation and evolution of the South China Sea. Geol. J. Chin. Univer. 13 (2), 311–322 (in Chinese with English Abstract).

Yan, P., Deng, H., Liu, H., Zhang, Z., Jiang, Y., 2006. The temporal and spatial distribution of volcanism in the South China Sea region. J. Asian Earth Sci. 27, 647–659.

Yan, Q.S., Shi, X.F., Wang, K.S., Bu, W.R., Xiao, L., 2008a. Major element, trace element, Sr–Nd–Pb isotopic studies of Cenozoic alkali basalts from the South China Sea. Sci. China (Ser. D) 51 (4), 550–566.

Yan, Q.S., Shi, X.F., Yang, Y.M., Wang, K.S., 2008b. K–Ar/Ar–Ar Geochronology of Cenozoic alkali basalts from the South China Sea. Acta Oceanol. Sin. 27 (6), 115–123.

Yan, Q.S., Shi, X.F., Wang, K.S., Liu, X.M., 2008c. LA-ICPMS dating of zircon U–Pb and tectonic significance of granitic rocks from Nansha block, the South China Sea. Acta Geol. Sin. 82 (8), 1057–1067 (in Chinese with English Abstract).

Yan, Q.S., Shi, X.F., Liu, X.M., Wang, K.S., Bu, W.R., 2010. Petrology and geochemistry of Mesozoic granitic rocks from the Nansha micro-block, the South China Sea: constraints on the basement nature. J. Asian Earth Sci. 37, 130–139.

Yan, Q.S., Shi, X.F., Li, N.S., 2011. Oxygen and lead isotopic characteristics of granitic rocks from the Nansha block (South China Sea): implications for their petrogenesis and tectonic affinity. Island arc 20, 150–159.

Yao, B.C., Wan, L., 2010. Variation of the lithospheric thickness in the South China Sea and its tectonic significance. Geol. China 37 (4), 888–899 (in Chinese with English Abstract).

Yao, B.C., Wan, L., Wu, N.Y., 2004. Cenozoic plate tectonic activities in the Great South China Sea area. Geol. China 31 (2), 113–122 (in Chinese with English Abstract).

Yu, J.H., O'Reilly, S.Y., Wang, L., Griffin, W.L., Zhang, M., Wang, R., Jiang, S., Shu, L., 2008. Where was South China in the Rodinia supercontinent? Evidence from U–Pb geochronology and Hf isotopes of detrital zircons. Precambr. Res. 164, 1–15.

Zartman, R., Haines, S., 1988. The plumbotectonic model for Pb isotopic systematics among major terrestrial reservoirs – a case for bidirectional transport. Geochim. Cosmochim. Acta 52, 1327–1339.

Zhang, L., Wang, K., Chen, Z., Liu, J., Yu, G., Wu, K., Lan, C., 1994. On "Cathaysia" – evidence from lead isotope study. Geol. Rev. 40, 200–208 (in Chinese with English Abstract).

Zhao, D., 2007. Seismic images under 60 hotspots: search for mantle plumes. Gondwana Res. 12, 335–355.

Zhou, X.M., Li, W.X., 2000. Origin of Late Mesozoic igneous rocks in southeastern China: implications for lithosphere subduction and underplating of mafic magmas. Tectonophysics 326, 269–287.

Zhou, P.B., Mukasa, S.B., 1997. Nb–Sr–Pb isotopic, and major- and trace-element geochemistry of Cenozoic lavas from the Khorat Plateau, Thailand: sources and petrogenesis. Chem. Geol. 137, 175–193.

Zhou, D., Liu, H., Chen, H., 2005. Mesozoic–Cenozoic magmatism in southern South China Sea and its surrounding areas and its implications to tectonics. Geotecton. Metallog. 29 (3), 354–363 (in Chinese with English abstract).

Zhou, D., Sun, Z., Chen, H.Z., Xu, H.H., Wang, W.Y., Pang, X., Cai, D.S., Hu, D.K., 2008. Mesozoic paleogeography and tectonic evolution of South China Sea and adjacent areas in the context of Tethyan and Paleo-Pacific interconnections. Island Arc 17, 186–207.

Zhou, H., Xiao, L., Dong, Y., Wang, C., Wang, F., Ni, P., 2009. Geochemical and geochronological study of the Sanshui basin bimodal volcanic rock suite, China: implications for basin dynamics in southeastern China. J. Asian Earth Sci. 34, 178–189.

Zhu, B.Q., Wang, H.F., 1989. Nd–Sr–Pb isotopic and chemical evidence for the volcanism with MORB-OIB source characteristics in the Leiqiong area, China. Geochemica 3, 193–201.

Zhu, B.Q., Wang, H.F., Mao, C.X., Zhu, N.J., Huang, R.S., Peng, J.H., Pu, Z.P., 1989. Geochronology and Nd–Sr–Pb isotopic evidence for mantle source in the ancient subduction zone beneath Sanshui basin, China. Chin. J. Geochem. 8, 65–71.

Zhu, B.Q., Wang, H.F., Chen, Y.W., Chang, X.Y., Hu, Y.G., Xie, J., 2004. Geochronological and geochemical constraint on the Cenozoic extension of Cathaysian lithosphere and tectonic evolution of the border sea basins in East Asia. J. Asian Earth Sci. 24, 163–175.

Ziegler, P.A., Cloetingh, S., 2004. Dynamic processes controlling evolution of rifted basins. Earth Sci. Rev. 64, 1–50.

Zindler, A., Hart, S.R., 1986. Chemical geodynamics. Ann. Rev. Earth Planet. Sci. 14, 493–571.

Zou, H.B., Fan, Q.C., 2010. U–Th isotopes in Hainan basalts: Implications for sub-asthenospheric origin of EM2 mantle endmember and the dynamics of melting beneath Hainan Island. Lithos 116, 145–152.

Zou, H.P., Li, P.L., Rao, C.T., 1995. Geochemistry of Cenozoic volcanic rocks in Zhujiangkou Basin and its geodynamic significance. Geochemica 24 (Suppl), 33–45 (in Chinese with English abstract).

Zou, H.B., Zindler, A., Xu, X.S., Qi, Q., 2000. Major and trace element, and Nd–Sr–Pb isotope studies of Cenozoic basalts in SE China: mantle sources, regional variations, and tectonic significance. Chem. Geol. 171, 33–47.